production because antibodies was not elevated in animals that had receive the therapeutic administration of plasmid DNAs as shown in a previous study (Matsumoto et al., 2004). In contrast to the relapse of biphasic EAE and chronic EAE, T cells may play a pivotal role in the development of acute EAE and the first attack of biphasic EAE. However, these findings do not exclude the possibility that T cells play a role in macrophage-dependent disease progression. Indeed, administration of anti-T cell monoclonal antibody suppressed the development of MOG-induced chronic EAE (our unpublished observation).

We determined the levels of macrophage-related chemokine mRNA in the spinal cord of rats during the relapse of biphasic and chronic EAE. Interestingly, the administration of 7ND, a dominant inhibitor of MCP-1/CCL2, suppressed both MCP-1/CCL2 and MIP-1α/CCL3 mRNA almost completely in the relapse of biphasic and chronic EAE. Although the precise mechanism by which the MCP-1/CCL2 inhibitor suppresses MIP-1α/CCL3 remains unknown, it was reported that 7ND suppresses a variety of cytokines and chemokines including IL-1β, RNATES, MIP-2 and IP-10 (Goser et al., 2005). Furthermore, pathological examinations revealed the marked decrease of macrophages in the lesions during the relapse of biphasic EAE (Table 3) and chronic EAE (Table 4). This may be attributable to general reduction of macrophage-related chemokines.

We also examined the levels of anti-MBP and anti-MOG antibodies in treated and control rats with three types of EAE. As clearly shown here, 7ND treatment ameliorated the clinical signs and pathology in some types of EAE without the downregulation of anti-neuroantigen antibodies. This finding suggests that 7ND exerts its function in a manner independent of the antibody production. However, this does not deny the role of anti-neuroantigen antibodies in chronic EAE and MS as demonstrated in previous studies (Lalive et al., 2006; Sakuma et al., 2004; von Budingen et al., 2002).

In summary, we have induced three different types of EAE in rats and treated them with the 7ND gene, a dominant inhibitor of MCP-1/CCL2, to elucidate the pathomechanisms of the lesion formation in EAE. Depending on the effect of the treatment in terms of the development of clinical signs and pathology, the lesion formation can be classified into two categories; i.e., T cell-dependent and macrophage-dependent lesion formations. These findings provide useful information to develop specific immunotherapies.

Acknowledgements

This study was supported in part by the Health and Labour Sciences Research Grants for Research on Psychiatric and Neurological Diseases and Mental Health and by Grants-in-Aid from the Japan Society for the Promotion of Science.

References

Agrawal, H.C., Burton, R.M., Fishman, M.A., Mitchell, R.F., Prensky, A.L., 1972. Partial characterization of a new myelin protein component. J. Neurochem. 19, 2083–2089.

Bar-Or, A., Oliveira, E.M., Anderson, D.E., Hafler, D.A., 1999. Molecular pathogenesis of multiple sclerosis. J. Neuroimmunol. 100, 252–259.

Bas, A., Forsberg, G., Hammarstrom, S., Hammarstrom, M.L., 2004. Utility of the housekeeping genes 18S rRNA, beta-actin and glyceraldehyde-3-phosphate-dehydrogenase for normalization in real-time quantitative reverse transcriptase-polymerase chain reaction analysis of gene expression in human T lymphocytes. Scand. J. Immunol. 59, 566–573.

Casado, V., Mallol, J., Bozal, J., 1988. Isolation and characterization of bovine brain myelin distribution of 5′-nucleotidase. Neurochem. Res. 13, 349–357.

Deibler, G.E., Martenson, R.E., Kies, M.W., 1972. Large scale preparation of myelin basic protein from central nervous tissue of several mammalian species. Prep. Biochem. 2, 139–165.

Egashira, K., 2003. Molecular mechanisms mediating inflammation in vascular disease: special reference to monocyte chemoattractant protein-1. Hypertension 41, 834–841.

Egashira, K., Koyanagi, M., Kitamoto, S., Ni, W., Kataoka, C., Morishita, R., Kaneda, Y., Akiyama, C., Nishida, K.I., Sueishi, K., Takeshita, A., 2000. Anti-monocyte chemoattractant protein-1 gene therapy inhibits vascular remodeling in rats: blockade of MCP-1 activity after intramuscular transfer of a mutant gene inhibits vascular remodeling induced by chronic blockade of NO synthesis. FASEB J. 14, 1974–1978.

Gong, J., Ratkay, L.G., Waterfield, J.D., Clark-Lewis, I., 1997. An antagonisit of monocyte chemoattractant protein 1 (MCP-1) inhibits arthritis in the MRL-*lpr* mouse model. J Exp. Med. 186, 131–137.

Goser, S., Ottl, R., Brodner, A., Dengler, T.J., Torzewski, J., Egashira, K., Rose, N.R., Katus, H.A., Kaya, Z., 2005. Critical role for monocyte chemoattractant protein-1 and macrophage inflammatory protein-1alpha in induction of experimental autoimmune myocarditis and effective anti-monocyte chemoattractant protein-1 gene therapy. Circulation 112, 3400–3407.

Huang, D.R., Wang, J., Kivisakk, P., Rollins, B.J., Ransohoff, R.M., 2001. Absence of monocyte chemoattractant protein 1 in mice leads to decreased local macrophage recruitment and antigen-specific T helper cell type 1 immune response in experimental autoimmune encephalomyelitis. J. Exp. Med. 193, 713–726.

Huitinga, I., Van Rooijen, N., De Groot, C.J.A., Uitdehaag, B.M.J., Dijkstra, C.D., 1990. Suppression of experimental allergic encephalomyelitis in Lewis rats after elimination of macrophages. J. Exp. Med. 172, 1025–1033.

Ikeda, Y., Yonemitsu, Y., Kataoka, C., Kitamoto, S., Yamaoka, T., Nishida, K., Takeshita, A., Egashira, K., Sueishi, K., 2002. Anti-monocyte chemoattractant protein-1 gene therapy attenuates pulmonary hypertension in rats. Am. J. Physiol. Heart Circ. Physiol. 283, H2021–H2028.

Jee, Y., Yoon, W.K., Okura, Y., Tanuma, N., Matsumoto, Y., 2002. Upregulation of monocyte chemoattractant protein-1 and CC chemokine receptor 2 in the central nervous system is closely associated with relapse of autoimmune encephalomyelitis in Lewis rats. J. Neuroimmunol. 128, 49–57.

Kennedy, K.J., Steir, R.M., Kunkel, S.L., Lukacs, N.W., Karpus, W.J., 1998. Acute and relapsing experimental encephalomyelitis are regulated by differential expression of the CC chemokines macrophage inflammatory protein-1α and monocyte chemotactic protein-1. J. Neuroimmunol. 92, 98–108.

Kim, G., Tanuma, N., Kojima, T., Kohyama, K., Suzuki, Y., Kawazoe, Y., Matsumoto, Y., 1998. CDR3 size spectratyping and sequencing of spectratype-derived T cell receptor of spinal cord T cells in autoimmune encephalomyelitis. J. Immunol. 160, 509–513.

Lalive, P.H., Menge, T., Delarasse, C., Della Gaspera, B., Pham-Dinh, D., Villoslada, P., von Budingen, H.C., Genain, C.P., 2006. Antibodies to native myelin oligodendrocyte glycoprotein are serologic markers of early inflammation in multiple sclerosis. Proc. Natl. Acad. Sci. U S A 103, 2280–2285.

Lassmann, H., 2004. Recent neuropathological findings in MS-implication for diagnosis and therapy. J. Neurol. Suppl. 4, IV/2–IV/5.

Lau, E.K., Paavola, C.D., Johnson, Z., Gaudry, J.P., Geretti, E., Borlat, F., Kungl, A.J., Proudfoot, A.E., Handel, T.M., 2004. Identification of the glycosaminoglycan binding site of the CC chemokine, MCP-1: implications for structure and function in vivo. J. Biol. Chem. 279, 22294–22305.

Lublin, F.D., Reingold, S.C., 1996. Defining the clinical course of multiple sclerosis: results of an international survey. Neurology 46, 907–911.

Lucchinetti, C., Brueck, W., Parisi, J., Scheithauer, B., Rodoriguez, M., Lassmann, H., 2000. Heterogeity of multiple sclerosis lesions: implication for the pathogenesis of demyelination. Ann. Neurol. 47, 707–717.

Matsumoto, Y., Fujiwara, M., 1987. The immunopathology of adoptively transferred experimental allergic encephalomyelitis (EAE) in Lewis rats.

Part 1. Immunohistochemical examination of developing lesion of EAE. J. Neurol. Sci. 77, 35–47.

Matsumoto, Y., Tsukada, Y., Miyakoshi, A., Sakuma, H., Kohyama, K., 2004. C protein-induced myocarditis and subsequent dilated cardiomyopathy: rescue from death and prevention of dilated cardiomyopathy by chemokine receptor DNA therapy. J. Immunol. 173, 3535–3541.

Matsumoto, Y., Sakuma, H., Miyakoshi, A., Tsukada, Y., Kohyama, K., Park, I., Naoyuki, T., 2005. Characterization of relapsing autoimmune encephalomyelitis and its treatment with decoy chemokine receptor gene. J. Neuroimmunol. 170, 49–61.

Ohmori, K., Hong, Y., Fujiwara, M., Matsumoto, Y., 1992. *In situ* demonstration of proliferating cells in the rat central nervous system during experimental autoimmune encephalomyelitis. Evidence suggesting that most infiltrating T cells do not proliferate in the target organ. Lab. Invest. 66, 54–62.

Proudfoot, A.E., Handel, T.M., Johnson, Z., Lau, E.K., LiWang, P., Clark-Lewis, I., Borlat, F., Wells, T.N., Kosco-Vilbois, M.H., 2003. Glycosaminoglycan binding and oligomerization are essential for the in vivo activity of certain chemokines. Proc. Natl. Acad. Sci. U S A 100, 1885–1890.

Sakuma, H., Kohyama, K., Park, I.K., Miyakoshi, A., Tanuma, N., Matsumoto, Y., 2004. Clinicopathological study of a myelin oligodendrocyte glycoprotein-induced demyelinating disease in LEW.1AV1 rats. Brain 127, 2201–2213.

Sospendra, M., Martin, R., 2005. Immunology of multipel sclerosis. Annu. Rev. Immunol. 23, 683–747.

Tran, E.H., Hoekstra, K., Van Rooijen, N., Dijkstra, C.D., Owens, T., 1998. Immune invasion of the central nervous system parenchyma and experimental allergic encephalomyelitis, but not leukocyte extravasation from blood, are prevented in macrophage-depleted mice. J. Immunol. 161, 3767–3775.

van der Goes, A., Boorsma, W., Hoekstra, K., Montagne, L., De Groot, C.J.A., Dijkstra, C.D., 2005. Determination of the sequential degradation of myelin protein by macrophages. J. Neuroimmunol. 161, 12–20.

von Budingen, H.C., Hauser, S.L., Fuhrmann, A., Nabavi, C.B., Lee, J.I., Genain, C.P., 2002. Molecular characterization of antibody specificities against myelin/oligodendrocyte glycoprotein in autoimmune demyelination. Proc. Natl. Acad. Sci. U S A 99, 8207–8212.

Zhang, Y., Rollins, B.J., 1995. A dominant negative inhibitor indicates that monocyte chemoattractant protein 1 functions as a dimer. Mol. Cell Biol. 15, 4851–4855.

Zhang, Y.J., Rutledge, B.J., Rollins, B.J., 1994. Structure/activity analysis of human monocyte chemoattractant protein-1 (MCP-1) by mutagenesis. Identification of a mutated protein that inhibits MCP-1-mediated monocyte chemotaxis. J. Biol. Chem. 269, 15918–15924.

Attenuation of Experimental Autoimmune Myositis by Blocking ICOS-ICOS Ligand Interaction[1]

Yasuhiro Katsumata,* Masayoshi Harigai,[2]*† Tomoko Sugiura,* Manabu Kawamoto,* Yasushi Kawaguchi,* Yoh Matsumoto,‡ Kuniko Kohyama,‡ Makoto Soejima,* Naoyuki Kamatani,* and Masako Hara*

Polymyositis (PM) is an acquired, systemic, connective tissue disease characterized by the proximal muscle weakness and infiltration of mononuclear cells into the affected muscles. To understand its etiology and immunopathogenesis, appropriate animal model is required. It has been demonstrated that immunization with native human skeletal C protein induces severe and reproducible experimental autoimmune myositis (EAM) in Lewis rats, and that the muscle inflammatory lesions in the EAM mimic those of human PM. In the present study, we prepared recombinant skeletal C protein fragment and succeeded in inducing as severe EAM as that by native C protein. We found ICOS expression on muscle fiber-infiltrating T cells in the EAM rats, but not in normal rats. Treatment with anti-ICOS mAb reduced incidence and severity of myositis; decreased the number of muscle-infiltrating CD11b/c$^+$, TCR$^+$, and CD8a$^+$ cells; and inhibited the expression of IL-1α and CCL2 in the hamstring muscles of the EAM rats. However, the treatment neither inhibited serum anti-C protein IgG level, C protein-induced proliferation of lymph node (LN) cells, or LN T cells, nor production of IFN-γ by C protein-stimulated LN cells in EAM rats. These data indicate that analysis of C protein-induced EAM provides not only insights into pathogenesis of PM, but also useful information regarding development of effective immunotherapy against the disease. ICOS-ICOS ligand interaction would be a novel therapeutic target for PM. *The Journal of Immunology,* **2007, 179: 3772–3779.**

Polymyositis (PM)[3] is an acquired, systemic, connective tissue disease characterized by the clinical and pathologic effects of chronic muscle inflammation (1). Although the etiology and much about the pathogenesis of PM remain elusive, it has increasingly been appreciated that in the muscles of patients with PM, clonally expanded CD8$^+$ CTLs invade muscle fibers that express MHC class I Ags (2, 3), which leads to fiber necrosis via the perforin pathway (4). However, no specific target Ags have been identified, and an agent initiating self-sensitization remains unknown (1). Although corticosteroid is the first-line drug for PM and most patients respond to it to some degree and for some time, others become steroid resistant and the addition of an immunosuppressive drug may become necessary (1).

Experimental autoimmune myositis (EAM) is an animal model for human idiopathic inflammatory myopathies and has served for the elucidation of the pathomechanism of the disease and the development of immunotherapy. Kohyama and Matsumoto (5) previously induced severe and reproducible EAM in Lewis rats by immunization with human skeletal C protein, and demonstrated that muscle inflammatory lesions mimicked those of human PM. C protein is a single polypeptide chain of 140 kDa present in thick filaments of skeletal and cardiac muscles (6). Its physiological function remains obscure, but thick filament structural support and conformational change during muscle activation have been suggested (6). However, the low purity of native C protein could result in the unstable myositis-inducing ability, and it is practically difficult to obtain highly purified native C protein at a sufficient amount for the induction of EAM in a large number of rats. The similar technical problem has been pointed out, and Matsumoto et al. (7) have recently prepared recombinant cardiac C protein and succeeded in inducing severe experimental autoimmune myocarditis in Lewis rats by immunization with the protein.

ICOS is a member of CD28 family costimulatory receptor expressed on activated T cells, and its ligand, ICOS ligand (ICOSL)/B7 homologous protein, belongs to B7 family. The human ICOS is 62–67% identical with rat ICOS, and 68% to mouse ICOS in amino acid sequence. The expression level of rat ICOS on T cells was relatively low, but its expression was drastically induced by the treatment with PMA plus Ca ionophore or the engagement of TCR/CD3 complex (8). Integration of signals through ICOS and other CD28 family receptors and their ligands is critical for activation of immune responses and induction of tolerance (9). Treatment with anti-ICOS or anti-ICOSL mAb ameliorated several animal models of autoimmune diseases, suggesting implication of ICOS-ICOSL interaction in their pathomechanisms. These included myosin-induced experimental autoimmune myocarditis in Lewis rats (10), proteolipid protein (PLP)-induced experimental allergic encephalomyelitis in SJL mice (11), type II collagen-induced arthritis in DBA/1J mice (12), and the murine lupus nephritis in NZB/W F_1 mice (13). It has also been reported that normal muscle fibers constitutively express low levels of ICOSL, whereas

*Institute of Rheumatology, Tokyo Women's Medical University, Tokyo, Japan; †Departments of Pharmacovigilance and Medicine and Rheumatology, Graduate School, Tokyo Medical and Dental University, Tokyo, Japan; and ‡Department of Molecular Neuropathology, Tokyo Metropolitan Institute for Neuroscience, Tokyo, Japan

Received for publication July 31, 2006. Accepted for publication July 10, 2007.

The costs of publication of this article were defrayed in part by the payment of page charges. This article must therefore be hereby marked *advertisement* in accordance with 18 U.S.C. Section 1734 solely to indicate this fact.

[1] This study was supported in part by grants-in-aid from the Japan Society for the Promotion of Science; the Ministry of Health, Labor, and Welfare, Japan; and the Ministry of Education, Science, Sports and Culture, Japan.

[2] Address correspondence and reprint requests to Dr. Masayoshi Harigai, Department of Pharmacovigilance, Tokyo Medical and Dental University, 1-5-45 Yushima, Bunkyo-ku, Tokyo 113-8519, Japan. E-mail address: mharigai.mpha@tmd.ac.jp

[3] Abbreviations used in this paper: PM, polymyositis; EAM, experimental autoimmune myositis; FCM, flow cytometry; ICOSL, ICOS ligand; LN, lymph node; PLP, proteolipid protein; rh, recombinant human.

 0022-1767/07/$2.00

muscle fibers in patients with inflammatory myopathies express markedly increased ICOSL expression (14). These observations led us to investigate effects of ICOS blockade in C protein-induced EAM in Lewis rats.

In the present study, we prepared recombinant skeletal C protein and induced EAM with the Ag to overcome the above problems. In addition, we analyzed the expression of ICOS in the muscles to clarify the pathomechanisms of the C protein-induced EAM in more detail and administered anti-ICOS mAb to the EAM rats to evaluate possible therapeutic value of ICOS blockade. Analysis of C protein-induced EAM provides not only insights into pathogenesis of human PM, but also useful information regarding development of effective immunotherapies against the disease.

Materials and Methods

Animals and proteins

Lewis rats were purchased from Charles River Laboratories and bred in our animal facility. Rats used in the present study were 6 wk old. Partially purified and purified skeletal myosin and native C protein were prepared, as described previously (5). The experimental protocol was approved by the Institutional Animal Care and Use Committee of Tokyo Women's Medical University.

Preparation of recombinant C protein fragments

Because C protein is too large to prepare recombinant protein as a whole protein, we planned to produce four protein fragments designated as fragments 1, 2, 3, and 4, corresponding to the 1–290, 284–580, 567–877, and 864-1142 aa sequences, respectively. Total RNA was isolated from human skeletal muscle using RNAzol B (Biotecx Laboratories) and then reverse transcribed into cDNA using ReverTra Ace-α- (Toyobo). Then cDNA was PCR amplified with KOD DNA polymerase (Toyobo) and fragment-specific primer pairs. Each primer was designed to possess the restriction enzyme site at both ends. PCR products were inserted into a cloning vector, pCR4 Blunt-TOPO in the Zero Blunt TOPO kit (Invitrogen Life Technologies), and clones with right sequences were obtained by the standard method. Several clones were subcloned into an expression vector, pQE30 (Qiagen), and used for large-scale preparation of C protein fragments. Recombinant C protein fragments produced in transformed *Escherichia coli* were isolated under denaturing conditions and purified using Ni-NTA agarose (Qiagen). Then purified protein fragments were diluted and refolded in 100 mM Tris-HCl (pH 8.0) containing 500 mM L-arginine, 2 mM glutathione (reduced form), 0.2 mM glutathione (oxidized form), and 2 mM EDTA, after which they were concentrated and dialyzed in PBS. As a final step, recombinant protein fragments were incubated with Detoxi-Gel (Pierce) overnight to remove endotoxins. Obtained protein fragments contained endotoxins <10 EU/1 mg protein, as determined with Toxinometer ET-2000 (WAKO). Because preliminary study demonstrated that fragment 2 had the highest water solubility among the four fragments and showed same ability to induce EAM as whole human C protein (5) (data not shown), we used fragment 2 in the following experiments.

Preparation of anti-ICOS Ab

Anti-rat ICOS mAbs (JmAb49 and JmAb50) and isotype-matched control IgG1κ mAb against keyhole limpet hemocyanin (JmAb216) were prepared at JT Frontier Research Laboratory, as described previously (15). JmAb49 was used for immunohistochemistry, and JmAb50 was used for in vivo experiments.

EAM induction and tissue sampling

Lewis rats were immunized by s.c. injection of the recombinant human (rh) C protein fragments with CFA (2.5 mg/ml *Mycobacterium tuberculosis*) in hind footpads, tail base, and neck one time each on a weekly basis, and were sacrificed 2 wk after the last immunization. For controls, PBS/CFA was injected according to the same protocol. To prevent degeneration of the Ags, only freshly prepared or short-term preserved (1 mo or less at −80°C) preparations were used. At the time of immunization, each rat received an i.p. injection of 2 μg of pertussis toxin (Seikagaku Kogyo). Rat muscles were removed from proximal portion of lower extremities and snap frozen in chilled isopentane precooled in liquid nitrogen on day 28. Rat inguinal lymph nodes (LNs) and spleen were also removed from each rat on day 28.

Treatment by anti-ICOS mAb

To study effects of anti-ICOS mAb on this animal model, we administered JmAb50 (3 mg/kg) or control mAb (JmAb216) (3 mg/kg) i.v. twice per week for 3 consecutive wk (days 7, 10, 14, 17, 21, and 24) to the rats along with the immunization by rhC protein fragment 2. All of the rats were sacrificed on day 28, and muscles, inguinal LNs, and spleen were removed from each rat, as described above.

Histological grading of inflammatory lesions and immunohistochemistry

For histological and immunohistological study, frozen sections (5 μm) were cut in a cryostat and air dried. For histological study, they were fixed in ether for 10 min and stained with H&E. Using H&E-stained sections, histological severity of inflammation was graded into the following four categories: grade 1, single or <5 muscle fiber involvement in one muscle block; grade 2, a lesion involving 5–30 muscle fibers in one muscle block; grade 3, a lesion involving a muscle fasciculus; grade 4, a diffuse extensive lesion. When multiple lesions were found in one muscle block, 0.5 was added to the score (5).

For immunohistochemical analysis, the biotin-free immunohistochemical staining through use of the HRP-labeled polymer system, without cross-reactivity with the rat specimen, was conducted according to the manufacturer's instructions (Histofine Simple Stain Rat MAX-PO (mouse; rabbit); Nichirei) (16). In brief, frozen sections were air dried and fixed in ether (at room temperature) or acetone (at −20°C) for 10 min. After a wash with PBS and incubation with normal goat or rabbit serum for 30 min, serial sections were incubated for 60 min at room temperature with primary mouse anti-rat mAbs, followed by the polymer-conjugated anti-mouse or rabbit IgG (Nichirei), and washed with PBS. For the substrate-chromogen reaction, diaminobenzidine tetrahydrochloride (Nichirei) was used according to the manufacturer's protocol. Control sections were subjected to the isotype-matched normal mouse IgG. Sections were counterstained with hematoxylin for 1 min and washed in tap water for 10 min. The mouse mAbs used in the present study for immunohistochemistry were R73 (1:1000 = 1 μg/ml; anti-TCR$\alpha\beta$; Serotec), W3/25 (1:400 = 2.5 μg/ml; anti-CD4; Cedarlane Laboratories), OX-8 (1:100 = 10 μg/ml; anti-CD8a; Oxford Biotechnology), OX42 (1:1000 = 1 μg/ml; anti-CD11b/c used as anti-macrophage; Oxford Biotechnology), JmAb49 (50 μg/ml; anti ICOS), OX18 (1 μg/ml; anti-MHC class I; Abcam), 3D6 (1 μg/ml; anti-MHC class II; Abcam), and goat anti-rat IL-1α (1/200 dilution; Santa Cruz Biotechnology). To evaluate the severity of inflammation in addition to the above mentioned histological grading, we counted the number of CD11b/c$^+$, TCR$^+$, and CD8a$^+$ cells in serial sections according to the method of Suzuki et al. (17). The evaluation of histological inflammatory changes was performed in a blind fashion for the experimental group identity.

Cell isolation protocol

Isolated piece of muscles was minced into 2- to 4-mm pieces with sterile scissors. The tissue pieces were added to cold DMEM (Nikken) supplemented with 10% heat-inactivated FBS (Sigma-Aldrich), 1% penicillin, and 1% streptomycin on ice; washed two to three times; and then incubated in collagenase type II (1 mg/ml) (Worthington Biochemical) dissolved in DMEM at 37°C for 2 h, mixing intermittently. The cells were gently dispersed by pipeting. The cell suspension was filtered through fine nylon mesh and washed two to three times. Cells were resuspended in DMEM, and cell yield and viability were measured. Single-cell suspensions of LN cells and splenocytes were prepared by passing through fine nylon mesh in DMEM supplemented with 10% heat-inactivated FBS, 1% penicillin, 1% streptomycin, and 5×10^{-5} M 2-ME. RBC were depleted by incubating in hypotonic solution (0.83% NH_4Cl, 20 mM Tris-HCl (pH 7.6)) at 37°C to prepare splenocytes.

Flow cytometric analysis of muscle cells and LN cells

mAbs against the following Ags were used for flow cytometry analysis: CD3 (G4.18, mouse IgG3), CD4 (OX-38, mouse IgG2a), CD8a (OX-8, mouse IgG1), and ICOS (JmAb49). All FITC-, PE-, or PerCP-conjugated mAbs and control Ig were obtained from BD Pharmingen. Anti-ICOS mAb (JmAb49) was biotinylated in our laboratory and was detected by streptavidin-PerCP (BD Biosciences). Multicolor analysis was performed using flow cytometry (FCM). Rat muscle cells or LN cells were washed three times in ice-cold FCM buffer (PBS-0.1% BSA-0.1% sodium azide). Cells were then incubated at 4°C with saturating amounts of the fluorochrome (i.e., FITC- or PE-)- or biotin-conjugated mAb for 30 min. Cells were washed twice in ice-cold FCM buffer and incubated at 4°C with streptavidin-PerCP for 30 min when necessary. After incubation, cells were washed three times in ice-cold FCM buffer and fixed in PBS containing 1%

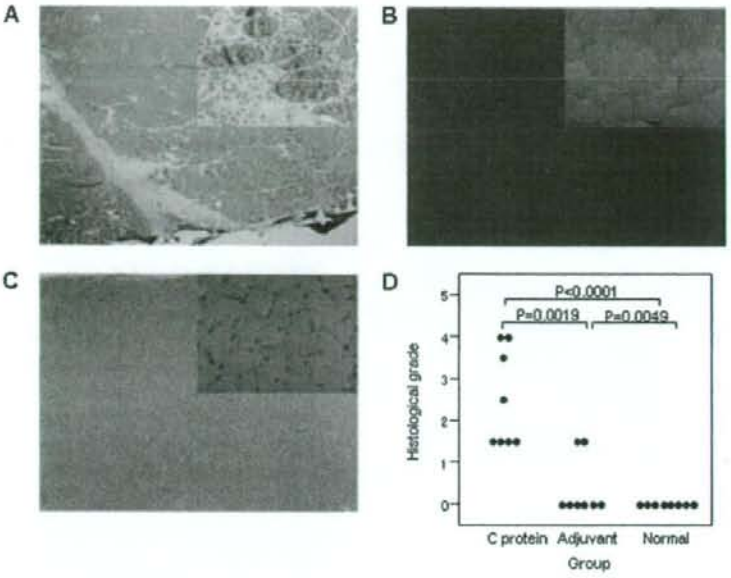

FIGURE 1. Histopathological features of EAM rats. Lewis rats were immunized on days 0, 7, and 14 with rhC protein fragment 2 and sacrified on day 28. *A*, Immunization with rhC protein fragment 2 elicited obvious EAM. *B* and *C*, Most muscle specimens from adjuvant-treated rats (*B*) and normal rats (*C*) showed normal appearance with neither inflammatory foci nor necrosis. *A–C*, H&E staining. Original magnification, ×40 (*A–C*) and ×400 (*inset* of *A–C*). *D*, Evaluation of myositis by the histological grades among rhC protein-immunized rats, adjuvant-treated rats, and normal rats. The histological grades of the rhC protein fragment 2-immunized rats were significantly higher than those of adjuvant-treated rats and normal rats. ●, The histological grade of one muscle (hamstrings) of each rat. Data represent the mean ± SEM values of eight muscles of four animals.

paraformaldehyde. The expression of cell surface markers was evaluated using an EPICS ALTRA (Beckman Coulter) cell sorter and EXPO32 analysis software (Beckman Coulter).

Quantitative PCR

Total RNA was extracted from freshly isolated muscle using TRIzol (Invitrogen Life Technologies) and was reverse transcribed to cDNA using SuperScript II RNase H^- (Invitrogen Life Technologies). One microliter of the cDNA was used as templates for quantitative PCR, which was performed using the ABI PRISM 7900HT Sequence Detection System (Applied Biosystems) with ΔΔCt method, according to the instructions of the manufacturer. Primers and probes for quantitative RT-PCR of rat GAPDH, IL-1α, and CCL2/MCP-1 were also purchased from Applied Biosystems.

Proliferation assay by rhC protein-stimulated LN cells and LN T cells

LN cells and splenocytes were prepared, as described above. OX-52 (pan T cell)-positive LN T cells of EAM rats were purified using mAb-conjugated microbeads and magnetic cell separation columns (Miltenyi Biotec). An APC-enriched population was prepared from normal rat splenocytes by depleting OX-52-positive T cells and HIS24 (CD45R)-positive B cells using MACS. Purified LN T cells (8×10^4) from EAM rats and 2×10^4 APC-enriched normal splenocytes were cocultured in 96-well culture plates in DMEM supplemented with 10% heat-inactivated FBS, 1% penicillin, 1% streptomycin, and 5×10^{-5} M 2-ME with various concentrations of denatured (60°C, 30 min) rhC protein fragment 2 for 72 h, and pulsed with [^{3}H]thymidine (1 μCi/well; Amersham Biosciences) for the last 8 h. Con A was added to some wells as a positive control for stimulation. [^{3}H]Thymidine incorporation was measured using Matrix96 (Packard Instrument).

ELISA for IFN-γ

Concentration of IFN-γ in the culture supernatant was measured using an ELISA kit (Amersham Biosciences), according to the protocol provided by the manufacturer.

ELISA for serum anti-C protein Ab

IgG anti-rhC protein fragment 2 Ab levels in the sera of EAM rats and normal rats were measured using ELISA, according to the protocol described below. A 96-well microtiter plate was coated with the rhC protein fragment 2 used for the induction of EAM and incubated at 4°C overnight. After incubation with normal calf serum at room temperature for 2 h, appropriately diluted rat serum samples were added. The plate was allowed to react with biotinylated goat anti-rat Ig $F(ab')_2$ (BioSource International) at room temperature for 2 h, followed by HRP-labeled streptavidin (Sigma-Aldrich) at room temperature for 60 min. The reaction was visualized using ABTS Microwell Peroxidase Substrate System (Kirkegaard & Perry Laboratories), and color development was measured at 415 nm by a Benchmark microplate reader (Bio-Rad).

Statistical analysis

Data are expressed as the mean ± SEM. Significant differences between the experimental groups were evaluated using Fisher's exact test (for the incidence of myositis), Mann-Whitney's *U* test (for the histological grades, the number of muscle-infiltrating $CD11b/c^+$, TCR^+, or $CD8a^+$ cells and quantitative RT-PCR), Student's unpaired *t* test (for the [^{3}H]thymidine incorporation and the concentration of IFN-γ), or Dunnett's test (for the serum anti-C protein Ab). All statistical analyses were performed using JMP statistical software (version 5.1.2; SAS Institute). Values of $p < 0.05$ were considered statistically significant.

Results

Histological grading of inflammatory lesions and immunohistochemistry

As representatively shown in Fig. 1*A*, immunization with fragment 2 of rhC protein elicited obvious EAM, the pathology of which is essentially the same as that induced with purified whole human native C protein, as previously reported (5). In the inflammatory foci of hamstrings and quadriceps muscles of rhC protein-immunized rats, numerous mononuclear cells were present in the endomysium and perimysium, and around the blood vessels in some fasciculuses. These cells often surrounded, invaded, and replaced the muscle fibers. Some muscle fibers were atrophic or necrotic and had internal nuclei. In moderate to severe inflammatory lesions, several muscle fibers were infiltrated with a large number of mononuclear cells. On the contrary, most muscle specimens from the control rats showed normal appearance with neither inflammatory foci nor necrosis, but some adjuvant-treated rats had a scatter of mononuclear cell infiltrates in the endomysium (Fig. 1, *B* and *C*). We also compared the histological grades among rhC protein-immunized rats, adjuvant-treated rats, and normal rats. The histological grades of the rhC protein-immunized rats were significantly higher than those of adjuvant-treated rats and normal rats (Fig. 1*D*).

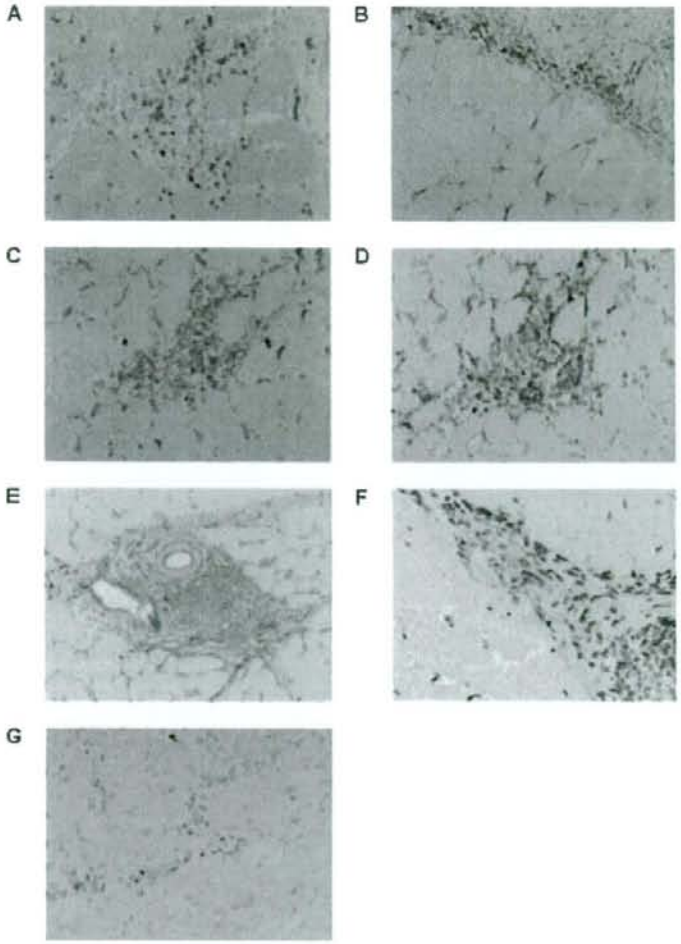

FIGURE 2. Immunohistochemical examinations during the acute phase of rhC protein-induced EAM. Lewis rats were immunized on days 0, 7, and 14 with rhC protein fragment 2, and sacrificed on day 28. Muscle tissues were analyzed by immunohistochemistry. *A*, Anti-TCR mAb-positive T cells were mainly located in the endomysium and some infiltrated muscle fibers. *B*, Very few $CD4^+$ cells (T cells and macrophages) infiltrated muscle fibers, although there were many $CD4^+$ cells in the endomysium. *C*, $CD8a^+$ T cells were the dominant infiltrating mononuclear cells of muscle fibers. *D*, A huge number of $OX42^+$ cells (macrophages) was recognized in both muscle fibers and the endomysium. *E*, MHC class I Ag^+ cells were located in the perivascular area and the endomysium. The vascular endothelial cells also expressed MHC class I Ag. *F*, MHC class II^+ cells were mainly found in the perimysium. *G*, Infiltrating mononuclear cells in the perivascular area and the perimysium as well as the vascular endothelial cells were positive for IL-1α. Original magnification, $\times 200$ (*A–G*).

To characterize the inflammatory cells in rhC protein-induced EAM, an immunohistochemical study was performed using a panel of mAbs (Fig. 2). As shown in Fig. 2*A*, anti-TCR mAb-positive T cells were mainly located in the endomysium and some infiltrated muscle fibers. Interestingly, very few $CD4^+$ cells (T cells and macrophages) infiltrated muscle fibers, although there were many $CD4^+$ cells in the endomysium (Fig. 2*B*). The total number of $CD8a^+$ T cells was small in comparison with that of $CD4^+$ cells. However, the numbers of $CD8a^+$ cells infiltrating muscle fibers were larger than those of $CD4^+$ cells (Fig. 2*C*). A huge number of $OX42^+$ cells (i.e., $CD11b/c^+$ macrophages) was recognized in both muscle fibers and the endomysium (Fig. 2*D*). These results were also very similar to those with whole native C protein, as previously reported (5). MHC class I Ag^+ mononuclear cells were located in the perivascular area as well as in the endomysium (Fig. 2*E*). The vascular endothelial cells also expressed MHC class I Ag, but the muscle fibers did not. MHC class II Ag^+ cells were mainly found in the perimysium (Fig. 2*F*). Because C protein-induced myositis in murine was IL-1 dependent (18), we evaluated the expression of IL-1α in rat EAM. Infiltrating mononuclear cells in the perivascular area and the perimysium as well as the vascular endothelial cells were positive for IL-1α (Fig. 2*G*), but not for TNF-α (data not shown).

ICOS expression in the inflammatory lesions of EAM rats

We next examined the expression of ICOS in muscles of EAM rats by immunohistochemistry. ICOS was expressed on some of muscle fiber-infiltrating mononuclear cells in EAM rats (Fig. 3, *A* and *B*), but not in normal rats; those cells were considered to be T cells by staining of serial sections (data not shown).

Expression of ICOS on T cells in the muscles of EAM rats was analyzed by flow cytometry. ICOS was expressed on 18.7–68.2% of CD3-positive T cells in the muscle of an EAM rat (Fig. 3*C*). Because few mononuclear cells infiltrated into muscles of normal rats, we could not perform flow cytometry analysis of these rats.

Anti-ICOS Ab therapy attenuated the disease progression of EAM

Because immunohistological examination suggested that ICOS might play an important role in the immunopathogenesis of EAM and treatment with anti-ICOS mAb ameliorated several animal models of autoimmune diseases, we explored the therapeutic effects of anti-ICOS mAb in our EAM rats. In these experiments, we used anti-ICOS mAb, JmAb50, which has been shown to inhibit binding of ICOS to ICOSL in vitro (15). EAM were induced by the immunization with rhC protein fragment 2, and anti-ICOS mAbs

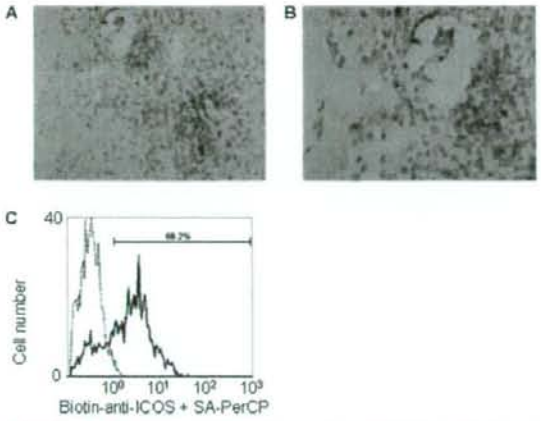

FIGURE 3. Expression of ICOS in muscles of EAM rats. Lewis rats were immunized on days 0, 7, and 14 with rhC protein fragment 2 and sacrificed on day 28. *A* and *B*, Expression of ICOS was examined by immunohistochemistry (original magnification, ×200 and ×400, *A* and *B*, respectively). ICOS was expressed on some of muscle fiber-infiltrating mononuclear cells in EAM rats. *C*, Single-cell suspension of muscles was obtained, as described in *Materials and Methods*, and the cells were stained with FITC-conjugated anti-CD3 mAb and biotinylated anti-ICOS mAb (JmAb49, solid line) or biotinylated control mAb (JmAb216, dotted line) with streptavidin (SA)-PerCP. CD3-positive cells were gated and analyzed. ICOS was expressed on 68.2% of CD3-positive T cells in the muscle of this EAM rat by flow cytometry analysis.

(JmAb50) or control mAb (JmAb216) (3 mg/kg) were administered i.v., as described in *Materials and Methods*. The muscles of control mAb-treated rats (Fig. 4*A*) showed severe inflammation, whereas the muscles of anti-ICOS mAb-treated rats showed only marginal inflammation (Fig. 4*B*). In the control group, the histological grade was 2.6 ± 0.23 and incidence of myositis was 100% (n = 14 muscles of 7 rats). The histological grade of anti-ICOS mAb-treated rats (0.9 ± 0.25) and incidence of myositis (n = 14 muscles of 7 rats, 57%) were significantly lower than those of controls (Fig. 4*C*) (p = 0.0001 and 0.0158, respectively). Similar results were obtained in two other independent set of experiments to treat EAM rats with anti-ICOS mAb (data not shown). To confirm the therapeutic effects of the treatment with anti-ICOS mAb, we performed an immunohistochemical analysis. Numbers of TCR$\alpha\beta^+$, CD8a$^+$, and CD11b/c$^+$ cells in the muscles of the anti-ICOS mAb-treated rats were significantly lower than those of the control mAb-treated rats (Fig. 4*D*). These findings clearly indicate that treatment with anti-ICOS mAb ameliorated myositis in EAM rats. We also examined the effects of anti-ICOS mAb treatment on the expression of IL-1α and CCL2 in the hamstring muscles of the EAM rats using quantitative RT-PCR. The expression of IL-1α and CCL2 mRNA in the anti-ICOS mAb-treated EAM rats was significantly lower than that in the control mAb-treated rats (Fig. 4*E*). IL-1α and CCL2 were not detected in the hamstring muscle of normal mice (data not shown). Taken together, these results strongly indicate that the treatment with anti-ICOS mAb ameliorated the C protein-induced EAM.

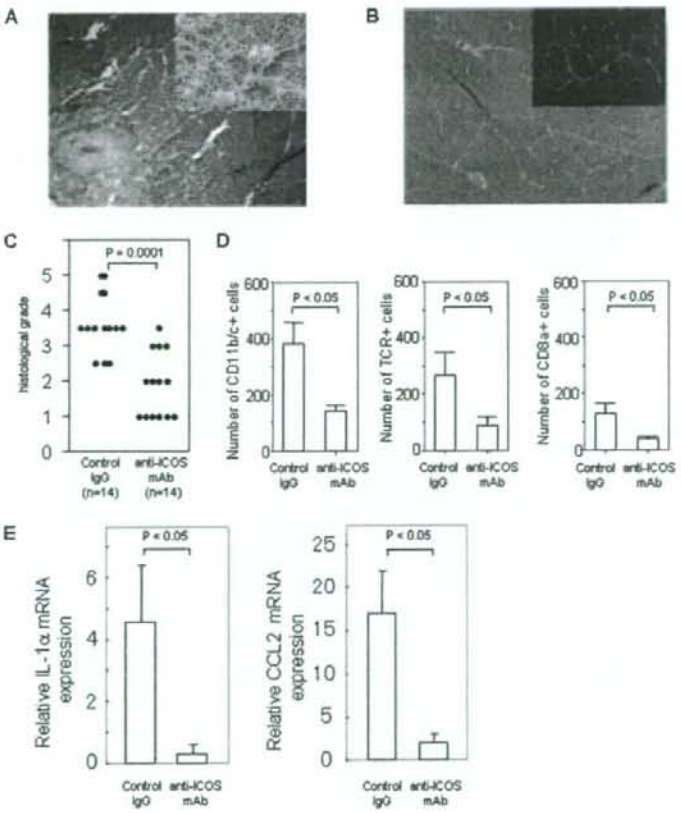

FIGURE 4. Effect of treatment with anti-ICOS mAb on EAM. Rats were immunized with rhC protein fragment 2, as described in *Materials and Methods*; given 3 mg/kg anti-ICOS mAb (JmAb50) or isotype-matched control mAb i.v. 7, 11, 14, 18, 21, and 25 days after the first immunization; and sacrificed on day 28. *A* and *B*, Representative findings of the muscles taken from a control IgG-treated C protein-induced EAM rat (*A*) and an anti-ICOS mAb-treated EAM rat (*B*). The muscles of control rats showed as severe inflammation as untreated EAM rats, whereas the muscles of anti-ICOS mAb-treated rats showed only marginal inflammation at most. *A* and *B*, H&E staining. Original magnification, ×40 (*A* and *B*) and ×400 (*inset* of *A* and *B*). *C*, ●, The histological grade of one muscle (hamstrings) of each rat (n = 14 for each treatment group). The data shown are representative of three independent experiments with similar results. *D*, Decreased numbers of infiltrating cells of each subset by anti-ICOS mAb treatment. Numbers of CD11b/c$^+$, TCR$^+$, and CD8a$^+$ cells were counted in the hamstring muscles from the control mAb-treated and anti-ICOS mAb-treated EAM rats. *E*, Reduction of IL-1α and CCL2 expression by anti-ICOS mAb treatment in the hamstring muscles of the EAM rats. IL-1α and CCL2 mRNA was measured using quantitative RT-PCR. Data represent the mean ± SEM (*D* and *E*).

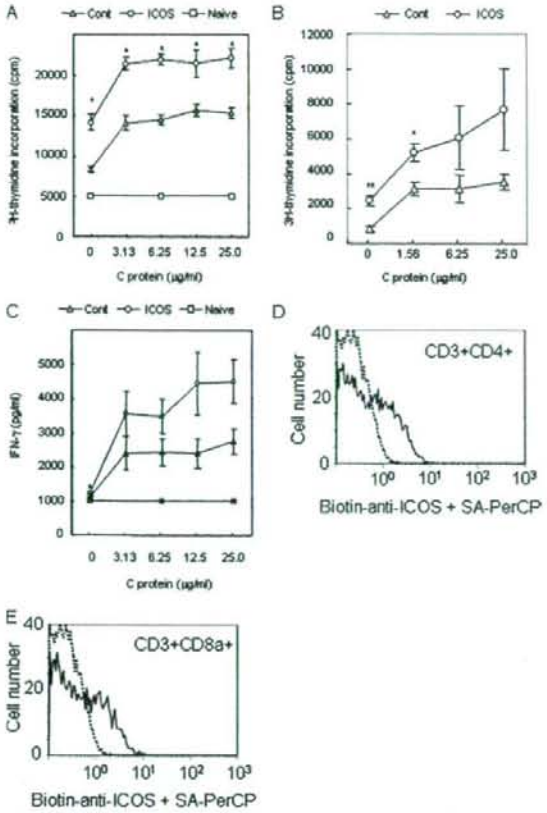

FIGURE 5. Effect of anti-ICOS mAb treatment on proliferation and IFN-γ production by LN cells and LN T cells. *A* and *B*, rhC protein-induced EAM rats were treated with control mAb (Δ) or anti-ICOS mAb (○), as described in Fig. 4, and LN cells (*A*) or LN T cells (*B*) were prepared on day 28. LN cells were also prepared from untreated naive rats (□, *A*). LN cells (1×10^5 cells/well) (*A*) or LN T cells (8×10^4 cells/well) and APC-enriched splenocytes (2×10^4 cells/well) from untreated naive rats (*B*) were cultured in the presence or absence of the indicated concentration of rhC protein fragment 2 for 72 h and pulsed with [^{3}H]thymidine for the last 8 h, and the incorporated radioactivity was measured. *C*, The supernatants of LN cells after a 72-h culture were assessed for IFN-γ production by ELISA. All data were shown as the mean ± SEM of seven mice in each group (the number of naive rats is 3) (*A* and *C*) or three mice (*B*). Data are representative of three independent experiments with similar results. *, $p < 0.05$; **, $p < 0.01$ (using Student's *t* test). *D* and *E*, LN cells from the control mAb-treated EAM rats were analyzed for the expression of ICOS using triple-color staining (FITC anti-CD3 mAb, PE anti-CD4 mAb (*D*), or PE anti-CD8a mAb (*E*), and biotinylated anti-ICOS mAb (JmAb49, solid line) or biotinylated control mAb (JmAb216, dotted line) and streptavidin (SA)-PerCP) and flow cytometry. $CD3^+CD4^+$ cells (*D*) or $CD3^+CD8a^+$ cells (*E*) were gated and analyzed for the expression of ICOS. Both $CD3^+CD4^+$ (*D*) and $CD3^+CD8a^+$ (*E*) T cells of control mAb-treated EAM rats expressed ICOS ($CD4^+$, 22.9%; $CD8a^+$, 22.6%).

Effect of ICOS inhibition on cellular immunity against C protein

To evaluate the effect of the treatment with anti-ICOS mAb (JmAb50) on cellular immunity, we examined Ag-induced proliferation of LN cells and LN T cells in EAM rats. LN cells as well as LN T cells from untreated EAM rats proliferated in response to rhC protein fragment 2 in a dose-dependent manner, whereas LN cells from naive rats did not proliferate even at a high concentration of the Ag (Fig. 5, *A* and *B*). Unexpectedly, the [^{3}H]thymidine incorporation of both LN cells and LN T cells from the anti-ICOS mAb-treated EAM rats was higher than that of control IgG-treated EAM rats, and the difference reached statistical significance at all the concentrations of rhC protein fragment 2 examined in LN cells (Fig. 5*A*) and at 0 and 1.56 μg/ml in LN T cells (Fig. 5*B*). Similar results were obtained in another independent set of experiments.

We also measured IFN-γ production of LN cells stimulated with rhC protein fragment 2. LN cells from naive rats did not produce IFN-γ in both the presence and absence of C protein (<8 pg/ml, data not shown). IFN-γ was produced at low levels by unstimulated LN cells of both control mAb-treated EAM rats and anti-ICOS mAb-treated rats, and the treatment with anti-ICOS mAb increased the mean levels of IFN-γ production without stimulation ($n = 7$ in each group) (Fig. 5*C*). Stimulation with rhC protein fragment 2 up-regulated the production of IFN-γ by the LN T cells from both treatment groups. The mean levels of IFN-γ production of anti-ICOS mAb-treated rats were higher than those of control mAb-treated rats, but the difference did not reach statistical significance ($n = 7$ in each group). Similar results were obtained in another independent set of experiments (data not shown). We also analyzed the inhibitory effect of the anti-ICOS mAb in vitro. C protein-specific proliferation of LN cells or LN T cells was not inhibited by the addition of JmAb50 (data not shown).

We prepared LN cells from both treatment groups and analyzed the expression of ICOS using triple-color staining (FITC anti-CD3 mAb, PE anti-CD4 mAb, or PE anti-CD8a mAb, and biotinylated JmAb49 and streptavidin-PerCP) and flow cytometry. Both $CD4^+$ and $CD8a^+$ T cells of control mAb-treated EAM rats expressed ICOS ($CD4^+$ T cells, 22.9–39.9%; $CD8a^+$ T cells, 23.5–26.0%) (Fig. 5, *D* and *E*), whereas those of anti-ICOS mAb-treated rats were very low ($CD4^+$ T cells, 2.8–5.9%; $CD8a^+$ T cells, 2.5–3.3%).

Effect of ICOS inhibition on humoral immunity against C protein

We next examined effect of anti-ICOS mAb on EAM by studying the humoral immune response. To evaluate the effect of the treatment with anti-ICOS mAb (JmAb50) on humoral immunity, sera taken at the end of the treatment were subjected to ELISA using rhC protein fragment 2. Anti-C protein Ab were markedly elevated in control IgG-treated EAM rats (0.984 ± 0.0403) than unimmunized normal rats (0.286 ± 0.0376) ($p < 0.05$) or adjuvant-treated rats (0.257 ± 0.0262) ($p < 0.05$), whereas levels of anti-C protein Ab in anti-ICOS mAb-treated EAM rats (0.839 ± 0.0734) were not significantly different from those of control IgG-treated EAM rats ($p = 0.12$).

These results suggest that treatment with anti-ICOS mAb did not affect the above aspects of humoral and cellular immunity against rhC protein 2 in EAM rats.

Discussion

The major findings of the present study were as follows: 1) skeletal rhC protein fragment 2 induced as severe myositis as native skeletal whole C protein in Lewis rats; 2) treatment with anti-ICOS mAb reduced incidence of myositis, with amelioration of histopathological features of myositis and reduction of IL-1α and CCL2 expression in EAM rats; and 3) treatment with anti-ICOS mAb did not affect serum anti-C protein Ab levels, and it unexpectedly enhanced the proliferative responses of LN cells and LN T cells to the Ag. Because ICOS blockade provided only histological improvement and the reduction of the expression of cytokine and chemokine, the clinical significance of the treatment remains unclear and requires further investigation.

We induced severe and reproducible EAM in Lewis rats by immunization with skeletal rhC protein fragment 2 and demonstrated that muscle fiber-infiltrating cells in the EAM were mainly $CD8a^+$ T cells and macrophages. Muscle inflammatory region of patients with PM is characterized by $CD8^+$ CTLs invading muscle fibers (1–3). The histopathological features of muscle inflammatory regions and type of muscle fiber-infiltrating cells in the EAM are similar to those of human PM, and thus the C protein-induced EAM could be served as a model for human PM. However, some of the pathological features of the EAM in rats are distinct from PM. Not only $CD8a^+$ T cells, but also many $OX42^+$ macrophages infiltrated muscle fibers in this model, whereas in humans, macrophages infiltrate muscle fibers less frequently in PM in comparison with toxic, necrotizing, or dystrophic myopathies (facioscapulohumeral; due to deficiency of dystrophin or dysferlin) in which macrophages predominate (1). Recently, Sugihara et al. (18) reported C protein-induced myositis in murine, which also shared several common histological features with human PM, including abundant infiltration of CD8 and perforin-expressing cells in the affected muscle.

For optimal stimulation, naive T cell requires the following two signals: the first one is provided by MHC-TCR interaction, and the second one is provided by costimulatory ligand and receptor pairs (19, 20). Muscle fibers do not express the classic costimulatory molecules B7-1 (CD80) or B7-2 (CD86) (21); instead, they express at least three costimulatory molecules, CD40 (22), BB-1 (21), and ICOSL (14). We previously demonstrated that CD40 was expressed on muscle cells, whereas CD154, the ligand of CD40, was expressed on muscle-infiltrating T cells in patients with PM/dermatomyositis, and that the expression of CD40 could be induced by the treatment with IFN-γ in vitro (22). Stimulation of human muscle cells with rCD154 enhanced production of IL-6, IL-8, and MCP-1 (22). BB-1 is one of the receptors for CD28 and CTLA-4, and the MHC-I/BB1-positive muscle fibers make direct cell-to-cell contact with the infiltrating $CD8^+$ cells via CD28 or CTLA-4 on their surface (21, 23). The results of the present study and the expression of ICOSL in patients with PM and other inflammatory myopathies (14) indicate that the ICOS-ICOSL interaction may also serve as costimulatory pairs for muscle-infiltrating T cells and may be involved in the pathogenesis of inflammatory myopathies.

To investigate immunological mechanisms of the treatment with anti-ICOS mAb (JmAb50), we measured rhC protein fragment 2-induced LN cell and LN T cell proliferation and IFN-γ production and serum anti-rhC protein fragment 2 IgG levels. Unexpectedly, none of them was inhibited by the treatment with JmAb50. In other animal models of autoimmune diseases, blockade of ICOS-ICOSL interaction inhibited proliferation of T cells, production of cytokines, and Ag-specific Ab levels, which would explain the beneficial effects of the treatment (10–13). However, we found that biotinylated anti-ICOS mAb (JmAb49) bound to LN T cells from the control mAb-treated EAM rats (Fig. 5, *D* and *E*), but did not bind to those from anti-ICOS mAb-treated EAM rats. Because vascular endothelial cells (24) and muscle cells (14) were reported to express ICOSL, these observations supported the possibility that the treatment may hamper migration of activated T cells into muscles or proliferation and/or survival of effector T cells in muscles by inhibiting interaction between ICOS and ICOSL. Unfortunately, rat ICOSL cDNA has not been cloned and we could not perform further analysis in our animal model.

Although ICOS-ICOSL blockade has been shown to inhibit T cell responses in many animal models of autoimmune diseases (10–13), it enhanced T cell responses under some experimental conditions. Rottman et al. (11) induced experimental allergic encephalomyelitis in SJL mice with PLP, and found that ICOS blockade during the efferent immune response (9–20 days after immunization) abrogated the disease, but blockade during Ag priming (1–10 days after immunization) exacerbated it. Upon culture with PLP and compared with immunized controls, proliferation and production of IFN-γ of splenocytes were decreased by efferent blockade, but increased by priming blockade. We administered anti-ICOS mAb 7–24 days after the first immunization to the rats along with the immunization (7 and 14 days after the first immunization) because mild inflammation was already observed in the EAM muscles on day 7 (data not shown) and we considered that day 7 would be already in efferent immune response phase. Administration of anti-ICOS mAb from day 7 might be too early to decrease cellular immune response against the Ag, but it requires further investigation to assess this possibility.

In conclusion, skeletal rhC protein fragment 2 induced as severe EAM as whole native C protein in Lewis rats, and the treatment with anti-ICOS mAb ameliorated EAM. ICOS-ICOSL interaction would be a novel therapeutic target of PM. Analysis of C protein-induced EAM provides not only insights into pathogenesis of human PM, but also useful information regarding development of effective immunotherapies against the intractable disease.

Acknowledgments

We thank Dr. Katsunari Tezuka and Dr. Masashi Sasabuchi (JT Pharmaceutical Frontier Research Laboratories, Kanagawa, Japan) for providing anti-ICOS mAbs (JmAb49 and JmAb50). We also thank Drs. Hitoshi Kohsaka and Toshihiro Nanki (Tokyo Medical and Dental University, Tokyo, Japan) for their critical advice.

Disclosures

The authors have no financial conflict of interest.

References

1. Dalakas, M. C., and R. Hohlfeld. 2003. Polymyositis and dermatomyositis. *Lancet* 362: 971–982.
2. Engel, A. G., and K. Arahata. 1984. Monoclonal antibody analysis of mononuclear cells in myopathies. II. Phenotypes of autoinvasive cells in polymyositis and inclusion body myositis. *Ann. Neurol.* 16: 209–215.
3. Arahata, K., and A. G. Engel. 1988. Monoclonal antibody analysis of mononuclear cells in myopathies. V. Identification and quantitation of $T8^+$ cytotoxic and $T8^+$ suppressor cells. *Ann. Neurol.* 23: 493–499.
4. Goebels, N., D. Michaelis, M. Engelhardt, S. Huber, A. Bender, D. Pongratz, M. A. Johnson, H. Wekerle, J. Tschopp, D. Jenne, and R. Hohlfeld. 1996. Differential expression of perforin in muscle-infiltrating T cells in polymyositis and dermatomyositis. *J. Clin. Invest.* 97: 2905–2910.
5. Kohyama, K., and Y. Matsumoto. 1999. C-protein in the skeletal muscle induces severe autoimmune polymyositis in Lewis rats. *J. Neuroimmunol.* 98: 130–135.
6. Dennis, J. E., T. Shimizu, F. C. Reinach, and D. A. Fischman. 1984. Localization of C-protein isoforms in chicken skeletal muscle: ultrastructural detection using monoclonal antibodies. *J. Cell Biol.* 98: 1514–1522.
7. Matsumoto, Y., Y. Tsukada, A. Miyakoshi, H. Sakuma, and K. Kohyama. 2004. C protein-induced myocarditis and subsequent dilated cardiomyopathy: rescue from death and prevention of dilated cardiomyopathy by chemokine receptor DNA therapy. *J. Immunol.* 173: 3535–3541.
8. Tezuka, K., T. Tsuji, D. Hirano, T. Tamatani, K. Sakamaki, Y. Kobayashi, and M. Kamada. 2000. Identification and characterization of rat AILIM/ICOS, a novel T-cell costimulatory molecule, related to the CD28/CTLA4 family. *Biochem. Biophys. Res. Commun.* 276: 335–345.
9. Carreno, B. M., and M. Collins. 2002. The B7 family of ligands and its receptors: new pathways for costimulation and inhibition of immune responses. *Annu. Rev. Immunol.* 20: 29–53.
10. Futamatsu, H., J. Suzuki, H. Kosuge, O. Yokoseki, M. Kamada, H. Ito, M. Inobe, M. Isobe, and T. Uede. 2003. Attenuation of experimental autoimmune myocarditis by blocking activated T cells through inducible costimulatory molecule pathway. *Cardiovasc. Res.* 59: 95–104.
11. Rottman, J. B., T. Smith, J. R. Tonra, K. Ganley, T. Bloom, R. Silva, B. Pierce, J. C. Gutierrez-Ramos, E. Ozkaynak, and A. J. Coyle. 2001. The costimulatory molecule ICOS plays an important role in the immunopathogenesis of EAE. *Nat. Immunol.* 2: 605–611.
12. Iwai, H., Y. Kozono, S. Hirose, H. Akiba, H. Yagita, K. Okumura, H. Kohsaka, N. Miyasaka, and M. Azuma. 2002. Amelioration of collagen-induced arthritis by blockade of inducible costimulator-B7 homologous protein costimulation. *J. Immunol.* 169: 4332–4339.
13. Iwai, H., M. Abe, S. Hirose, F. Tsushima, K. Tezuka, H. Akiba, H. Yagita, K. Okumura, H. Kohsaka, N. Miyasaka, and M. Azuma. 2003. Involvement of

inducible costimulator-B7 homologous protein costimulatory pathway in murine lupus nephritis. *J. Immunol.* 171: 2848–2854.

14. Wiendl, H., M. Mitsdoerffer, D. Schneider, A. Melms, H. Lochmuller, R. Hohlfeld, and M. Weller. 2003. Muscle fibres and cultured muscle cells express the B7.1/2-related inducible co-stimulatory molecule, ICOSL: implications for the pathogenesis of inflammatory myopathies. *Brain* 126: 1026–1035.
15. Sakamoto, S., K. Tezuka, T. Tsuji, N. Hori, and T. Tamatani. 2001. AILIM/ICOS: its expression and functional analysis with monoclonal antibodies. *Hybrid Hybridomics* 20: 293–303.
16. Noiri, E., A. Nakao, K. Uchida, H. Tsukahara, M. Ohno, T. Fujita, S. Brodsky, and M. S. Goligorsky. 2001. Oxidative and nitrosative stress in acute renal ischemia. *Am. J. Physiol.* 281: F948–F957.
17. Suzuki, F., T. Nanki, T. Imai, H. Kikuchi, S. Hirohata, H. Kohsaka, and N. Miyasaka. 2005. Inhibition of CX3CL1 (fractalkine) improves experimental autoimmune myositis in SJL/J mice. *J. Immunol.* 175: 6987–6996.
18. Sugihara, T., C. Sekine, T. Nakae, K. Kohyama, M. Harigai, Y. Iwakura, Y. Matsumoto, N. Miyasaka, and H. Kohsaka. 2007. A new murine model to define the critical pathologic and therapeutic mediators of polymyositis. *Arthritis Rheum.* 56: 1304–1314.
19. Liang, L., and W. C. Sha. 2002. The right place at the right time: novel B7 family members regulate effector T cell responses. *Curr. Opin. Immunol.* 14: 384–390.
20. Krummel, M. F., and M. M. Davis. 2002. Dynamics of the immunological synapse: finding, establishing and solidifying a connection. *Curr. Opin. Immunol.* 14: 66–74.
21. Behrens, L., M. Kerschensteiner, T. Misgeld, N. Goebels, H. Wekerle, and R. Hohlfeld. 1998. Human muscle cells express a functional costimulatory molecule distinct from B7.1 (CD80) and B7.2 (CD86) in vitro and in inflammatory lesions. *J. Immunol.* 161: 5943–5951.
22. Sugiura, T., Y. Kawaguchi, M. Harigai, K. Takagi, S. Ohta, C. Fukasawa, M. Hara, and N. Kamatani. 2000. Increased CD40 expression on muscle cells of polymyositis and dermatomyositis: role of CD40-CD40 ligand interaction in IL-6, IL-8, IL-15, and monocyte chemoattractant protein-1 production. *J. Immunol.* 164: 6593–6600.
23. Murata, K., and M. C. Dalakas. 1999. Expression of the costimulatory molecule BB-1, the ligands CTLA-4 and CD28, and their mRNA in inflammatory myopathies. *Am. J. Pathol.* 155: 453–460.
24. Okamoto, N., Y. Nukada, K. Tezuka, K. Ohashi, K. Mizuno, and T. Tsuji. 2004. AILIM/ICOS signaling induces T-cell migration/polarization of memory/effector T-cells. *Int. Immunol.* 16: 1515–1522.

The American Journal of Pathology, Vol. 170, No. 1, January 2007

DOI: 10.2353/ajpath.2007.060544

Cardiovascular, Pulmonary and Renal Pathology

B-Cell Epitope Spreading Is a Critical Step for the Switch from C-Protein-Induced Myocarditis to Dilated Cardiomyopathy

Yoh Matsumoto, Il-Kwon Park, and Kuniko Kohyama

From the Department of Molecular Neuropathology, Tokyo Metropolitan Institute for Neuroscience, Tokyo, Japan

Repeated inflammation in the heart is one of the initiation factors of dilated cardiomyopathy (DCM). In a previous study, we established a new animal model for DCM by immunization of rats with recombinant cardiac C-protein fragment 2 (CC2). The present study examined factors involved in the development of DCM. Analysis using overlapping peptides revealed that the major carditogenic epitope resides only in the residue 615–647 [CC2 peptide 12 (CC2P12)]. However, immunization with CC2P12 induced moderate inflammation without subsequent DCM. CDR3 spectratyping analysis of the T-cell repertoire demonstrated that Vβ4-positive T cells were preferentially expanded in both CC2- and CC2P12-immunized rats. Although there was no significant difference in the T-cell characteristics, examinations of the B-cell epitope revealed that marked epitope spreading occurred in CC2-immunized but not CC2P12-immunized rats from 4 weeks after immunization. Consistent with this finding, immunization with CC2P12 and simultaneous transfer of anti-peptide antisera induced significantly more severe inflammation and fibrosis than CC2P12 immunization alone. However, the transfer of the antisera without CC2P12 immunization did not induce any pathology. These findings suggest that T-cell activation and B-cell epitope spreading in the CC2 molecule is a key step for the switch from myocarditis to the development of DCM. ***(Am J Pathol 2007, 170:43–51; DOI: 10.2353/ajpath.2007.060544)***

Dilated cardiomyopathy (DCM) is a serious and frequently fatal disorder and is a common cause of heart failure. The majority of DCM is sporadic, and mostly virus-induced immune mechanisms are suspected.[1] Because the heart biopsy sometimes demonstrates the presence of inflammation, several immunosuppressive therapies have been tried to improve the status of DCM.[2–4] However, significant progress has not been made, although these therapies have shown some improvements of the disease. Difficulties in finding effective therapies are mainly based on the fact that the pathogenesis of DCM is still poorly understood. The establishment of a suitable animal model that mimics human DCM and elucidation of pathogenesis of DCM will provide useful information for the development of effective therapies.

In a previous study, we demonstrated that cardiac C-protein, one of the myosin-binding proteins, induced severe experimental autoimmune carditis (EAC) and subsequent DCM in Lewis rats.[5] Seventy-five percent of rats immunized with C-protein died by day 50, and all of the survivors developed DCM. Furthermore, it was revealed that cytokines and chemokines produced by T cells and macrophages were up-regulated in the heart lesions, mainly during the inflammatory phase of EAC. These findings suggest that pathogenic T cells and possibly B cells play an important role in the development of EAC and subsequent DCM.

In the present study, we first examined the carditogenic epitopes that reside in the cardiac C-protein fragment 2 (CC2) (corresponding to amino acid residues 317–647). Using overlapping peptides, we found that only peptide 12 (CC2P12) possessed the carditis-inducing ability in the CC2 molecule. Interestingly, CC2P12 induced nonfatal moderate EAC and did not develop DCM. Analysis of clonally expanded T cells in CC2- and CC2P12-immunized rats demonstrated that there was no significant difference between the two groups. In contrast, CC2-immunized rats exhibited marked B-cell epitope spreading 4 weeks after immunization and afterward, whereas CC2P12-immunized rats raised antibodies only against CC2P12 and CC2. Based on these

Supported in part by grants-in-aid from the Japan Society for the Promotion of Science.

Accepted for publication September 14, 2006.

Address reprint requests to Yoh Matsumoto, Department of Molecular Neuropathology, Tokyo Metropolitan Institute for Neuroscience, Musashidai 2-6, Fuchu, Tokyo 183-8526, Japan. E-mail: matyoh@tmin.ac.jp.

Table 1. Amino Acid Sequences of Synthetic Peptides Encompassing CC2 Used in the Study

Peptide	Residue	Sequence
P1	317–348	AEEDVWEILRQAPPSEYERIAFQYGVTDLRGM
P2	344–375	DLRGMLKRLKGMRRDEKKSTAFQKKLEPAYQV
P3	371–402	PAYQVSKGHKIRLTVELADHDAEVKWLKNGQE
P4	398–429	KNGQEIQMSGSKYIFESIGAKRTLTISQCSLA
P5	425–456	QCSLADDAAYQCVVGGEKCSTELFVKEPPVLI
P6	452–483	PPVLITRPLEDQLVMVGQRVEFECEVSEEGAQ
P7	479–510	EEGAQVKWLKDGVELTREETFKYRFKKDGQRH
P8	506–537	DGQRHHLIINEAMLEDAGHYALCTSGGQALRE
P9	533–564	QALRELIVQEKKLEVYQSIADLMVGAKDQAVF
P10	560–591	DQAVFKCEVSDENVRGVWLKNGKELVPDSRIK
P11	587–619	DSRIKVSHIGRVHKLTIDDVTPADEADYSFVPE
P12	615–647	SFVPEGFACNLSAKLHFMEVKIDFVPRQEPPKI

C-protein fragment 2 encompasses amino acid 317–647 residues of human cardiac C-protein.

findings, we performed transfer experiments and demonstrated that both activation of T cells and anti-peptide antibody elevation are required for the initiation and subsequent progression of the disease. The present study strongly suggests that B-cell epitope spreading is an essential step for the switch from myocarditis to DCM.

Materials and Methods

Animals and Proteins

Lewis rats were purchased from SLC Japan (Shizuoka) and bred in our animal facility. Seven- to 11-week-old male and female rats were used.

Preparation of Recombinant C-Protein Fragments and Synthetic Peptides

The preparation of recombinant C-protein was precisely described previously.[5] Polymerase chain reaction (PCR) products corresponding to fragments 1, 2, 3, and 4 were inserted into a cloning vector, pCR4 Blunt-TOPO in the Zero Blunt TOPO kit (Invitrogen, Groningen, The Netherlands), and clones with correct sequences were subcloned into an expression vector, pQE30 (Qiagen, Tokyo, Japan). Then, recombinant C-protein fragments produced in transformed *Escherichia coli* were isolated under denaturing conditions and purified using Ni-NTA Agarose (Qiagen).

Synthetic peptides encompassing CC2, designated as CC2P1-CC2P12 (Table 1), were synthesized using a peptide synthesizer (Shimadzu, Kyoto, Japan). All of the peptides used in this study were >90% pure as determined and were purified if necessary using HPLC.

Conjugation of CC2P12 with KLH

To increase immunogenicity of CC2P12, the peptide was conjugated with keyhole limpet hemocyanin (KLH; Wako, Tokyo, Japan) as described previously.[6] KLH (in 0.083 mol/L sodium phosphate, 0.9 mol/L NaCl, and 0.1 mol/L ethylenediamine tetraacetic acid, pH 7.2) and *m*-maleimidobenzoyl-*N*-hydrosuccinimide ester in dimethyl sulfoxide (MBS; Pierce, Chicago, IL) at concentrations of 10 and 20 mg/ml, respectively, were incubated at a ratio of 10:1 for 1 hour at room temperature. Then, excess MBS was removed on a HiTrap desalting column (Amersham Biosciences, Tokyo, Japan). Finally, the KLH-CC2P12 complex was formed by incubating MBS-KLH with CC2P12 for 2 hours at room temperature.

EAC Induction and Tissue Sampling

Lewis rats were immunized once on day 0 with the indicated antigen with complete Freund's adjuvant (CFA) (2.5 mg/ml *Mycobacterium tuberculosis*) in the hind foot pads. At the time of immunization, rats received an intraperitoneal injection of 2 μg of pertussis toxin (PT; Seikagaku Corp., Tokyo, Japan). The numbers of rats used for experiments are shown in the footnotes of tables and the figure legends. Histological and immunohistochemical examinations were performed at the indicated time points using frozen and paraffin-embedded sections of the heart. Although evaluation of EAC and DCM was mainly based on histological examinations (see below), clinical score was also recorded: grade 1, dyspnea; grade 2, dyspnea plus ruffling of fur; and grade 3, moribund condition or death.

Histological Grading of Inflammatory Lesions and Immunohistochemistry

EAC inflammatory lesions were evaluated using hematoxylin and eosin (H&E)-stained sections according to the following criteria: grade 1, rare focal inflammatory lesions; grade 2, multiple isolated foci of inflammation frequently associated with pericarditis; grade 3, diffuse inflammation involving the outer layer of the muscle; grade 4, grade 3 plus focal transmural inflammation; and grade 5; diffuse inflammation with necrosis. CC2 immunization induced pericarditis that was frequently associated with pericardial and pleural effusion. However, we did not include the findings in the scores because the above grading system covered the whole range of mild to severe EAC. The extent of fibrosis revealed by Azan staining was graded into five categories: grade 1, rare scattered foci of fibrosis; grade 2, multiple isolated foci of fibrosis; grade 3, fibrosis involving the outer layer of the

muscle; grade 4, grade 3 plus partial transmural fibrosis; and grade 5, diffuse fibrosis.

Establishment of T-Cell Lines and the Proliferative Assay

CC2- or CC2P12-specific T-cell lines were established from draining (popliteal) lymph node cells taken from CC2- or CC2P12-immunized rats by cycle stimulations with CC2 or CC2P12 in the presence of mitomycin C-treated thymocytes as antigen-presenting cells. Between antigen stimulations, T cells were propagated in culture medium containing 5% Con A supernatant.

Proliferative responses of lymph node cells were assayed in microtiter wells by the uptake of [^{3}H]thymidine. After being washed with phosphate-buffered saline, lymph node cells (2×10^5 cells/well) were cultured with the indicated concentrations of CC2 or CC2 peptides for 3 days, with the last 18 hours in the presence of 0.5 μCi of [^{3}H]thymidine (Amersham Pharmacia Biotech, Tokyo, Japan). In some experiments, the proliferative responses of CC2- or CC2P12-specific T-cell lines (3×10^4 cells/well) were assayed in the presence of the antigens and antigen-presenting cells (5×10^5 cells/well). The cells were harvested on glass-fiber filters, and the label uptake was determined using standard liquid scintillation techniques.

CDR3 Spectratyping

CDR3 spectratyping was performed as described previously.[7,8] In brief, PCR products were added to an equal volume of formamide/dye loading buffer and heated at 94°C for 2 minutes. The amplified PCR products were electrophoresed on polyacrylamide sequencing gels, and the fluorescence-labeled DNA profile on the gels was directly recorded using an FMBIO fluorescence image analyzer (Hitachi, Yokohama, Japan). The presence or absence of contaminations of the reagents used in PCR was examined every 10 PCR analyses by performing PCR without the templates. When contaminations were present, all reagents used and the results obtained during the period were discarded.

ELISA

The levels of anti-CC2 and anti-CC2 peptide antibodies were measured using the standard ELISA test. Recombinant CC2 and CC2P1-P12 (10 μg/ml) were coated onto microtiter plates, and serially diluted sera from normal and immunized animals were applied. After washing, appropriately diluted horseradish-conjugated anti-rat IgG, IgG1, or IgG2a was applied. The reaction products were then visualized after incubation with the substrate. The absorbance was read at 450 nm.

Generation of Polyclonal Antibodies Against CC2 and CC2 Peptides

Polyclonal antibodies against CC2 and CC2 peptides were raised by immunizing rats with the antigens/CFA four times on a weekly basis. Sera were obtained 1 week after the last immunization, and ammonium sulfate-precipitated preparations were used for the transfer experiments. The presence of antibodies against the indicated antigens was confirmed by ELISA.

Statistical Analysis

Unless otherwise indicated, Student's *t*-test or Mann-Whitney's *U*-test was used for the statistical analysis.

Results

Autoimmune Carditis-Inducing Ability of Recombinant C-Protein and Synthetic Peptides

As reported in our previous study,[5] recombinant CC2 (amino acid residues 317–647 of human cardiac C-protein) possessed the strongest carditogenic activity among four recombinant proteins encompassing the entire molecule. In the present study, we prepared 12 overlapping synthetic peptides (Table 1) covering the CC2 molecule and examined their carditis-inducing ability. As shown in Table 2, we first screened all of the peptides using the peptide mixtures (groups A through D). Only mixture 4 containing peptides 10, 11, and 12 at 100 μg of each peptide (CC2P10 to -P12) induced EAC in all of the immunized rats (group D), whereas mixtures 1, 2, and 3 induced mild EAC in one of three rats (groups A through C). Then, we tested the carditogenicity of each peptide in mixture 4 and found that only peptide 12 (CC2P12) possessed a carditis-inducing ability (group G). However, it should be noted that compared with CC2, both inflammation and fibrosis induced with CC2P12 were significantly milder as estimated on day 17 and 6 weeks after immunization (group G versus group I). Because immunization with 300 μg of CC2P12 did not differ to 100 μg of CC2P12 immunization in terms of the histological severity, the pooled data are shown in Table 2. In addition, CC2P12-immunized rats did not develop DCM at 6 weeks postimmunization (PI) (see below). Another important aspect was the survival rate. As shown in Figure 1, 75% of the rats immunized with CC2 died of cardiac failure by day 50 PI. In sharp contrast, all of the rats immunized with CC2P12 had survived by day 50. Furthermore, CC2P12 was conjugated with KLH to increase the immunogenicity, and rats were immunized with the conjugate. However, this procedure did not augment the carditis-inducing ability of CC2P12 (group H). In an additional experiment, we immunized rats with a mixture of P1, P5, P8, P11, and P12, but the histological score was not significantly different from that of P12-immunized rats (data not shown). Collectively, these findings suggest that substances induced after CC2P12 immunization lack

Table 2. Histological Severities of EAC Induced by Immunization with the Peptide Mixtures, Synthetic Peptides, and Recombinant CC2*

Group	Antigen	Sampling	Incidence	Inflammation	Fibrosis
A	Mix 1 (P1 to P3)	3 weeks	1/3	0.7 ± 0.7	0
B	Mix 2 (P4 to P6)	3 weeks	1/3	0.3 ± 0.3	0
C	Mix 3 (P7 to P9)	3 weeks	1/3	0.2 ± 0.2	0
D	Mix 4 (P10 to P12)	3 weeks	3/3	2.5 ± 1.2	0
E	P10	Day 17	0/3	0†	0
F	P11	Day 17	1/3	0.2 ± 0.2†	0
G	P12	Day 17	4/4	2.0 ± 0.4†	0
		6 weeks	6/6	1.8 ± 0.4†	1.8 ± 0.6‡
H	P12-KLH	4 weeks	2/3	0.7 ± 0.3	0.7 ± 0.3
		6 weeks	3/3	1.3 ± 0.3†	0.8 ± 0.4‡
I	CC2	Day 17	5/5	4.1 ± 0.4†	1.5 ± 0.4
		6 weeks	6/6	3.8 ± 0.2†	4.1 ± 0.2‡

*Lewis rats were immunized once with mixtures 1, 2, 3, and 4 that had consisted of peptides 1 to 3, 4 to 6, 7 to 9, and 10 to 12, respectively (100 μg of each peptide), in CFA in the foot pads along with intraperitoneal injection of pertussis toxin (2 μg). Because mix 4 showed carditogenicity, each peptide in the mixture (P10, P11, and P12) was tested in a similar manner. For comparison, the results obtained with recombinant C-protein fragment 2 are also shown. The denominators in the incidence column represent the number of rats used for each experiment.

†Analysis of variance and multiple comparison (Scheffe's F-test) were performed, and significant differences were noted in the following combinations: P10 versus CC2, $P = 0.002$; P11 versus CC2, $P = 0.0001$; P12 versus CC2, $P = 0.008$ on day 17; P12 versus CC2, $P = 0.003$; P12-KLH versus CC2, $P = 0.003$ at 6 weeks.

‡Significant differences were noted in the following combinations: P12 versus CC2, $P = 0.011$; P12-KLH versus CC2, $P = 0.004$ at 6 weeks.

some aggravation factors for EAC/DCM induced by immunization with CC2.

Figure 2 depicts normal histology of the heart (A, D, G, and J) and pathology of EAC induced by CC2 (B, E, H, and K) and CC2P12 (C, F, I, and L). At 2 weeks PI, when EAC was at the acute inflammatory stage, the hearts taken from CC2-immunized rats showed marked hypertrophy (Figure 1B), whereas the hearts from CC2P12-immunized rats showed slight enlargement (Figure 1C). We measured the long and short axes of the middle portion of normal, CC2-immunized, and CC2P12-immunized rats and calculated the heart area at this level. As shown in Table 3, there were significant differences between normal and CC2-immunized rats ($P = 0.01$) and between CC2- and CC2P12-immunized rats ($P = 0.005$), indicating that the hearts from CC2-immunized rats showed marked hypertrophy. In contrast, there was no significant difference between the normal and CC2P12-immunized groups. H&E (Figure 2, E and F) and azan (Figure 2, H and I) stainings showed that compared with CC2-induced EAC (Figure 2, E and H), both inflammation and fibrosis were mild (Figure 2, F and I). In sections immunostained for macrophages, there was extensive and diffuse macrophage infiltration in CC2-induced EAC (Figure 2K), whereas macrophage infiltration in CC2P12-induced EAC was mild and focal (Figure 2L). B-cell infiltration was absent in both types of EAC (data not shown).

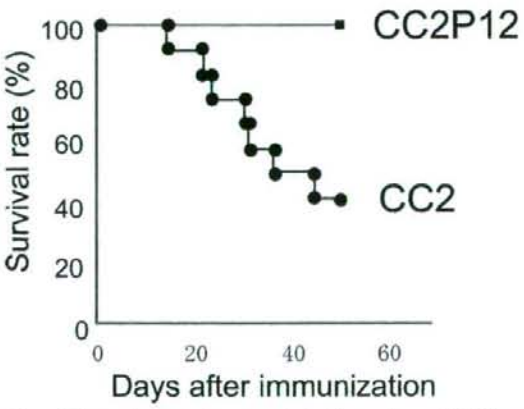

Figure 1. The survival rate of rats immunized with recombinant CC2/CFA or CC2P12/CFA with the intraperitoneal injection of pertussis toxin. Seventy-five percent of rats immunized with CC2 died between days 15 and 49 PI, whereas all of the rats immunized with CC2P12 survived during the observation period.

Characterization of Pathogenic T Cells

We next tried to determine whether a carditogenic peptide, CC2P12, contains an immunodominant or cryptic T-cell epitope. The representative results of three experiments are shown in Figure 3, A and B. When CC2 was immunized, the draining lymph node cells responded vigorously to CC2 but not to all of the overlapping peptide (P1 to P12 in Figure 3A). Similar experiments were performed using CC2-specific T-line cells after four to five cycles of antigen stimulation, and essentially the same results were obtained (data not shown). After CC2P12 immunization, lymph node cells responded well to CC2P12 and also to CC2 to a lesser extent (Figure 3B). These findings suggest that CC2P12 is processed and presented to T cells from CC2P12-immunized rats but is a cryptic epitope in the CC2 molecule for T cells from CC2-immunized rats.

In a previous study, we showed with CDR3 spectratyping analysis that in cardiac myosin-induced EAC, Vβ8.2 and Vβ10 TCR were clonally expanded in the inflamed heart and that Vβ8.2- and Vβ10-targeted immunotherapy was effective in ameliorating the severity of EAC.[7] We performed a similar analysis to characterize the nature of clonally expanded T cells in the heart with C-protein-induced EAC. The representative profiles are depicted in Figure 3, C and D, and all of the results are

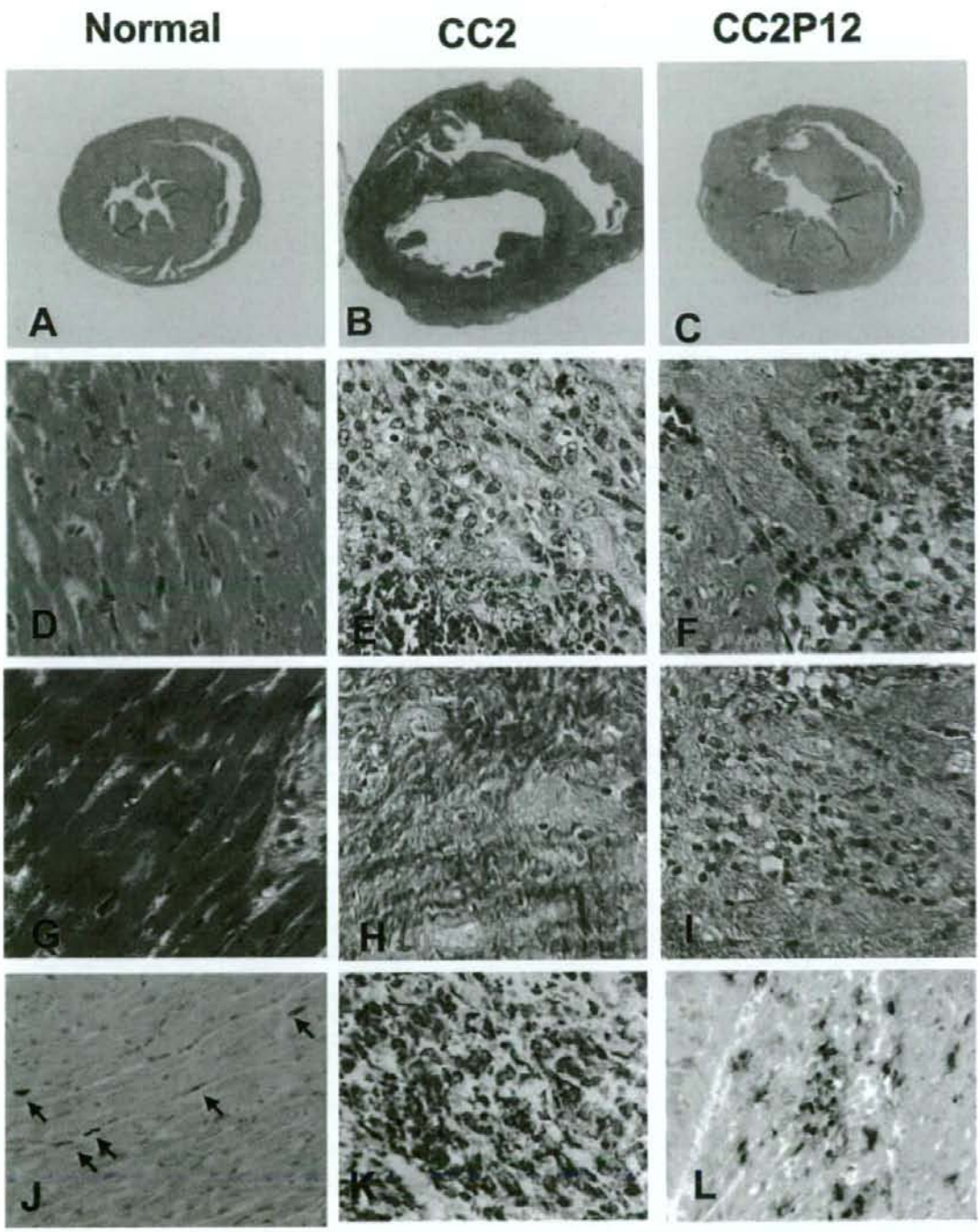

Figure 2. Normal histology (**A**, **D**, **G**, and **J**) and pathology of EAC induced by immunization with CC2 (**B**, **E**, **H**, and **K**) and CC2P12 (**C**, **F**, **I**, and **L**). At 2 weeks PI, when EAC was at the acute inflammatory stage, the hearts taken from CC2-immunized rats showed marked hypertrophy (**B**) compared with the normal heart (**A**), whereas the hearts from CC2P12-immunized rats showed only slight enlargement (**C**). H&E (**E** and **F**) and azan (**H** and **I**) stainings showed that compared with CC2-induced EAC (**E** and **H**), both inflammation and fibrosis of the heart were mild in CC2P12-immunized rats (**F** and **I**). In sections immunostained for macrophages, there was extensive and diffuse macrophage infiltration in CC2-induced EAC (**J**), whereas macrophage infiltration in CC2P12-induced EAC was mild and focal (**K**). **A–C:** H&E staining; the photographs were taken at the same magnification. **D–F:** H&E staining, ×240. **G–I:** Azan staining, ×240. **J–L:** ED1 staining, ×240.

Table 3. Measurements of Hearts under Normal and Diseased Conditions*

Condition	No. of rats examined	Diameter (mm)		Estimated area of hearts (mm^2)†
		Long axis	Short axis	
Normal	3	0.83 ± 0.10	0.72 ± 0.12	0.47 ± 0.14‡
CC2	6	1.20 ± 0.19	0.97 ± 0.08	0.91 ± 0.19‡
CC2P12	6	0.91 ± 0.08	0.80 ± 0.11	0.58 ± 0.13‡

*Rats were immunized once with CC2 or CC2P12, and the hearts were taken at 6 weeks after immunization. The long and short axes of the diameter were measured at the middle portion of the hearts. The hearts from CC2P12-immunized rats were measured before and after fixation, and those from normal and CC2-immunized rats were measured only after fixation. Because there was no significant change before and after fixation, all the values shown in the table are those measured after fixation.

†The heart area was calculated as long axis/2 × short axis × 3.14.

‡Significant differences were noted between normal and CC2-immunized rats ($P = 0.01$) and between CC2- and CC2P12-immunized rats ($P = 0.005$). However, there was no significant difference between normal and CC2P12-immunized rats.

summarized in Figure 3E. Infiltrating T cells in the heart of CC2-immunized rats on day 25 PI showed Vβ3 and Vβ4 expansion (Figure 3C, arrows), and those of CC2P12-immunized rats on day 17 PI showed Vβ4, Vβ8.6, and Vβ17 expansion (Figure 3D, arrows). The longitudinal study of CC2-immunized rats revealed interesting findings. On day 9 PI, T cells infiltrating the heart were rather heterogonous, and no particular Vβ expansion was noted (Figure 3E). In contrast, between days 14 and 28 PI when the inflammatory lesion reached at the maximal level,[5] Vβ4 expansion was detected in all of the cases examined. Other Vβs such as Vβ1, -7, -8.5, and -16 were expanded in one-half of the cases. Interestingly, T cells found in the heart at the later stage (6 and 10 weeks), when there was extensive fibrosis, showed the normal spectratype pattern (Figure 3E). These findings suggested that infiltrating T cells showing oligoclonal expansion play an important role in the development of EAC lesions (see the results of the transfer experiments below). However, T cells found at the later stage may be less involved in the disease progression. CDR3 spectratyping analysis of heart-infiltrating T cells of CC2P12-immunized rats was performed on day 17 and at 4 weeks PI and revealed that there was Vβ4 expansion in all of the cases examined. Taken together, Vβ4-positive T cells appear to play an important role in lesion formation in both CC2- and CC2P12-induced EAC, and there was no significant difference in the T-cell characteristics between the two groups.

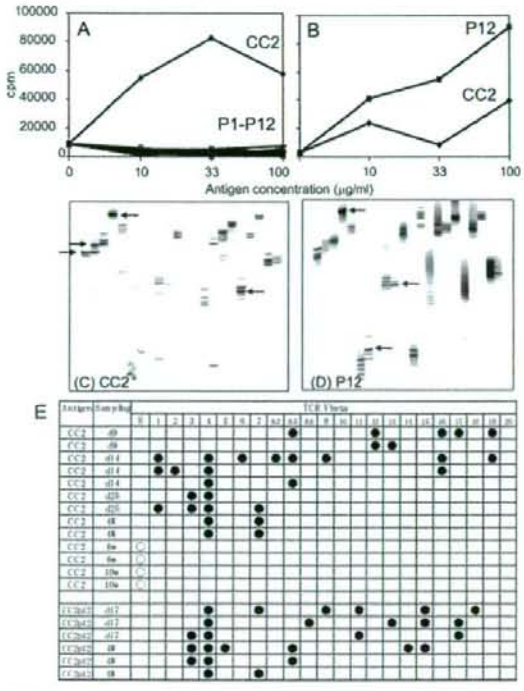

Figure 3. A and **B:** The proliferative responses of lymph node cells taken from CC2-immunized (**A**) and CC2P12-immunized (**B**) rats on day 12 PI. Lymph node cells (2×10^5 cells/well) were cultured with the indicated antigen for 72 hours, with the last 18 hours in the presence of [^{3}H]thymidine. The cells were harvested on glass-fiber filters, and the label uptake was determined using standard liquid scintillation techniques. Each symbol represents the mean value of triplicate assays, and SEMs were within 10% of the mean values. **C** and **D:** CDR3 spectratyping profiles of heart-infiltrating T cells taken from CC2-immunized (**C**) and CC2P12-immunized (**D**) rats. Marked spectratype expansions are indicated by **arrows**. **E:** Summary of the results of CDR3 spectratyping of T cells in the hearts from CC2- and CC2P12-immunized rats. Each line represents the result obtained from one rat. Closed circles represent Vβ clonal expansion. N, the normal spectratype pattern; w, weeks.

Characterization of Pathogenic B Cells and Anti-C-Protein Antibodies

As shown in Table 2 and Figure 2, CC2P12-immunized rats showed mild to moderate EAC without subsequent DCM. Moreover, unlike CC2-induced EAC, CC2P12-induced EAC was not fatal. These findings suggest that there are factors in CC2, but not in CC2P12, that aggravate EAC and induce DCM. Because we did not find clear differences between CC2- and P12-reactive T cells in the clonality analysis, we next examined the nature of antibodies raised by CC2 (Figure 4A) and CC2P12 (Figure 4B) immunization. From 1 to 12 weeks PI, sera were collected from CC2-immunized rats, and the levels of antibodies against CC2 and CC2P1 to -P12 were determined by ELISA (Figure 4A). At the early stage (1 to 3.5 weeks), only anti-CC2 antibodies were elevated in CC2-immunized rats. Then, anti-P8 and anti-P11 antibodies rose between 4 and 6 weeks, and some others showed at a high level thereafter. In one case examined at 12 weeks PI (4335 in Figure 4A), antibodies against all of the peptides were detected. This finding clearly showed that there was B-cell epitope spreading in CC2-immunized

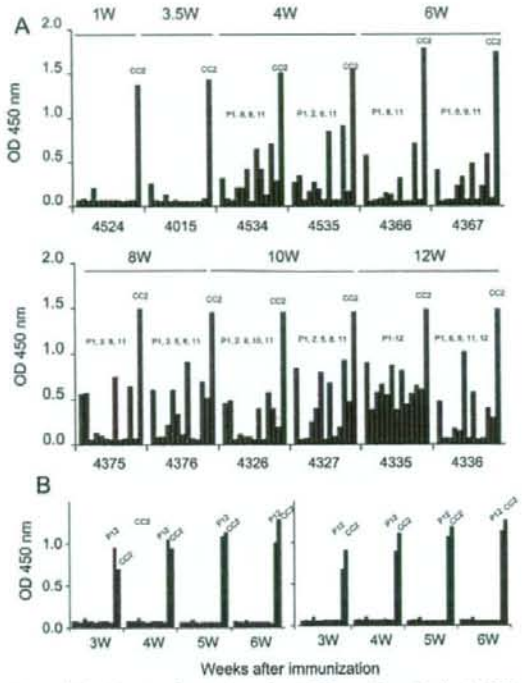

Figure 4. The kinetics of anti-CC2 and anti-CC2 peptide antibodies in CC2-immunized (**A**) and CC2P12-immunized (**B**) rats. **A:** The levels of anti-CC2 and anti-CC2 peptide antibodies were determined using ELISA. Recombinant CC2 and CC2P1-P12 (10 μg/ml) were coated onto microtiter plates, and diluted sera from CC2-immunized rats were applied. After washing, horseradish peroxidase-conjugated anti-rat IgG was allowed to react. The reaction products were then visualized after incubation with the substrate. The absorbance was read at 450 nm. **B:** The kinetics of anti-CC2 and anti-CC2 peptide antibodies in CC2P12-immunized rats. During the observation period, only anti-CC2P12 and anti-CC2 antibodies were elevated.

rats. Because this phenomenon was detected in the peripheral blood and there was no B-cell infiltration in the heart (data not shown), B-cell epitope spreading would take place in the lymphoid organ. In sharp contrast, in CC2P12-immunized rats, only antibodies against CC2P12 and CC2 were recognized in all of the rats examined by 6 weeks PI (Figure 4B).

CC2P12 Immunization and Cotransfer of Anti-CC2 or CC2 Peptide Antibodies Elicited Severe EAC

We further tried to identify factors that are responsible for the development of full-blown EAC and subsequent DCM. We already obtained the following findings. First, although CC2P12 was the sole carditis-inducing peptide in the CC2 molecule, CC2P12 induced relatively mild EAC without subsequent DCM. Second, there was no significant difference in the T-cell specificity between CC2-immunized and CC2P12-immunized rats. Finally, CC2-immunized rats showed marked intramolecular epitope spreading in the antibody production, whereas CC2P12-immunized rats developed antibodies that reacted with the immunizing antigen and the CC2 molecule. These findings raised the possibility that the generation of CC2-reacting T cells and generation of antibodies against various parts of the CC2 molecule are essential for full-blown EAC and subsequent DCM.

To test this possibility, we performed transfer experiments using various types of T cells and antibodies. The results are summarized in Table 4. Adoptive transfer of spleen and lymph node cells induced mild EAC in the recipients, whereas adoptive transfer of CC2-specific T-line cells did not elicit inflammation (Table 4, groups A and B). This finding suggests that not only T cells but also B cells are required for the development of inflammation in the heart. Cotransfer of anti-CC2 or anti-CC2P1–12 antisera after CC2P12 immunization aggravated both inflammation (Table 4, group D versus F, $P = 0.03$; group E versus F, $P = 0.005$) and fibrosis (Table 4, group D versus F, $P = 0.049$; group D versus F, $P = 0.01$) of EAC. There was no significant difference in the carditis-exacerbating ability between anti-CC2P1–12 and anti-CC2 antisera (Table 4, group D versus E). It should be noted that the transfer of anti-CC2 antisera alone did not induce EAC at all (group G). These findings strongly suggest that T cells are required for the initiation of inflammation in the heart and that anti-CC2 antibodies aggravate both inflammation and fibrosis.

Discussion

DCM is a serious problem for patients with heart failure because the disease progresses irreversibly and often ends in death. To develop effective therapies, it is essential to elucidate the pathomechanisms of the development of DCM. However, there are few good experimental models for DCM. In a previous study, we succeeded in inducing severe EAC with a high fatality rate and subsequent DCM in survivors by immunizing Lewis rats with cardiac C-protein.[5] This animal model is useful not only for the elucidation of the pathomechanisms of DCM but also for the development of effective immunotherapies.[5]

In the present study, we first tried to determine the carditis-inducing epitopes in the CC2 molecule and found that only peptide 12 (CC2P12), covering the residues 615–647, contains carditogenic epitope(s). Interestingly, immunization with CC2P12 induced moderate EAC but did not lead to subsequent DCM. Here, we demonstrated in a C-protein-induced animal model that B-cell epitope spreading occurred in CC2-immunized rats with DCM but not in CC2P12-immunized rats without DCM and that elevation of antibodies against various parts of the CC2 molecule is essential for the induction of more severe inflammation and fibrosis. However, it should be noted that activation of pathogenic T cells as demonstrated by CDR3 spectratyping is essential for the initiation of lesion formation because adoptive transfer of anti-CC2 antisera alone did not induce pathology at all.

Epitope spreading was first described in detail by Lehmann et al[9] as a key process for the development of chronic autoimmune encephalomyelitis. Initially, T-cell

Table 4. Summary of Cell and Antibody Transfer Experiments in EAC

Group	Immunization	Cell transfer		Ab transfer
		Cells	Dose	Ab
A	—	SpC + LNC*	10^7	—
B	—	CC2 TCL*	102 to 6×10^6	—
C	—	CC2P12 TCL*	3.5 to 6×10^6	—
D	CC2P12‡	—	—	Anti-P1-P12 sera
E	CC2P12‡	—	—	Anti-CC2 sera
F	CC2P12‡	—	—	Normal sera
G	—	—	—	Anti-CC2 sera

*CC2-reactive T cells or CC2P12 with or without antibodies were administered, and the degree of inflammation and fibrosis was evaluated 3 weeks after cell transfer. The denominators in the incidence column represent the number of rats used for each experiment. SpC, spleen cells; LNC, lymph node cells; TCL, T-cell line; —, not performed.

†n.e., not examined.

‡CC2P12 was immunized, and the indicated sera (1 ml after 5-fold dilution) were injected intravenously twice a week for 5 weeks. Rats were examined histologically 6 weeks after the immunization.

§Significant differences were noted in the following comparisons: D versus F, $P = 0.03$; E versus F, $P = 0.005$.

¶Significant differences were noted in the following comparisons: D versus F, $P = 0.049$; E versus F, $P = 0.01$.

(Table continues)

epitope spreading was intensively investigated, and this immunological event was thought to be highly involved in the relapse and chronicity of autoimmune diseases.[10–12] Later, it was reported that B-cell epitope spreading is also involved in the pathogenesis of autoimmune diseases.[13,14] Notably, Bischof et al[15] have shown that immunization of mice with myelin oligodendrocyte glycoprotein, but not with myelin basic protein and proteolipid protein, induced extensive B-cell epitope spreading and chronic autoimmune encephalomyelitis. Furthermore, they observed that diversification of the B-cell reactivity did not follow a sequential cascade that is seen in T-cell epitope spreading but represented a simultaneous spread toward a broad range of antigenic epitopes. In the present study, we also observed a similar mode of B-cell epitope spreading. Many reports have suggested that autoantibodies against cardiac components play an important role in the formation of DCM.[16–20] This assumption was also supported by the finding that immunoadsorption therapy to remove IgG ameliorated myocardial inflammation[4] and improved the cardiac performance and clinical status.[21] In addition, we have also observed that intravenous immunoglobulin administration suppressed the development of CC2-induced DCM and down-regulated anti-CC2 antibody production (our unpublished observation).

It is important to analyze the nature of DCM-inducing antibodies. We induced severe EAC with extensive fibrosis by immunization with CC2P12 plus transfer of anti-P1 to -P12 antisera that had been raised by peptide mixture immunization, but could not fully reconstitute the features of EAC and DCM produced by CC2 immunization. One of the reasons for this was that in our treatment protocol, it was difficult to maintain anti-peptide antibodies at a high level (unpublished observation). Although the reconstitution experiments demonstrated that anti-CC2P1–12 antisera possessed almost the same carditis-exacerbating ability as anti-CC2 antisera, there is a possibility that antibodies recognizing the conformational epitopes with high titers elicited by CC2 immunization but not by CC2P12 immunization are involved in the processes of DCM formation. In this regard, we are currently generating monoclonal antibodies against conformational epitopes of the CC2 molecule to test their ability of producing DCM. The conformational epitope mapping analysis would be helpful to identify pathogenic antibodies.

Increasing information about the pathogenesis of DCM will provide more chance for immunotherapies for the prevention and/or cessation of DCM. If pathogenic antibodies are identified more accurately, then specific and selective immunoadsorption could be achieved effectively with minimal side effects. In cases of DCM developed in a manner similar to that shown in the present study, intravenous immunoglobulin therapy, which is already in clinical trials,[22] is expected to be effective. Another important aspect is the timing of treatment initiation. As demonstrated in the previous[5] and present studies, histological examination revealed that fibrosis of the heart starts at 4 weeks PI and establishes at 6 to 8 weeks PI. Generation of the full range of pathogenic antibodies starts at the same period of time. Therefore, this time point is critical for the start of treatment. Improvements in the image analysis and functional studies are expected to greatly increase the effect of DCM therapy.

In summary, we identified the amino acid residue containing carditis-inducing epitope(s) in the CC2 molecule. By comparing CC2-induced EAC and subsequent DCM with peptide-induced EAC, it was demonstrated that B-cell epitope spreading is critical for the development of DCM. Importantly, by down-regulating pathogenic antibodies, it is possible to control the disease processes. Information obtained in the present study will provide useful information for the development of effective immunotherapies against human DCM.

Acknowledgment

We thank Y. Kawazoe for technical assistance.

Table 4. Continued

Ab transfer	Inflammation		Fibrosis	
Dose	Incidence	Grade	Incidence	Grade
—	2/2	2	n.e.†	n.e.
—	0/5	0	n.e.	n.e.
—	2/3	0.8 ± 0.6	0/3	0
5× dilution (1 ml) × 2/week × 5 weeks	3/3	3.3 ± 0.3§	3/3	3.3 ± 0.2¶
5× dilution (1 ml) × 2/week × 5 weeks	4/4	3.4 ± 0.3§	4/4	3.3 ± 0.3¶
5× dilution (1 ml) × 2/week × 5 weeks	4/4	1.5 ± 0.5§	4/4	1.6 ± 0.4¶
5× dilution (1 ml) × 2/week × 5 weeks	0/3	0	0/3	0

References

1. Liu PP, Mason JW: Advances in the understanding of myocarditis. Circulation 2001, 104:1076–1082
2. Parrillo JE, Cunnion RE, Epstein SE, Parker MM, Suffredini AF, Brenner M, Schaer GL, Palmeri ST, Cannon RO, Alling D, Wittes JT, Ferrnas VJ, Rodriguez ER, Fauci AS: A prospective, randomized, controlled trial of predonisone for dilated cardiomyopathy. N Engl J Med 1989, 321:1061–1068
3. Wojnicz R, Nowalany-Kozielska E, Wojciechowska C, Glanowska G, Wilczewski P, Niklewski T, Zembala M, Polonske L, Rozek MM, Wodniecki J: Randomized, placebo-controlled study for immunosuppressive treatment of inflammatory dilated cardiomyopathy. Circulation 2001, 104:39–45
4. Staudt A, Schaper F, Stangl V, Plagemann A, Bohm M, Merkel K, Wallukat G, Wernecke KD, Stangl K, Baumann G, Felix SB: Immunohistological changes in dilated cardiomyopathy induced by immunoadsorption therapy and subsequent immunoglobulin substitution. Circulation 2001, 103:2681–2686
5. Matsumoto Y, Tsukada Y, Miyakoshi A, Sakuma H, Kohyama K: C protein-induced myocarditis and subsequent dilated cardiomyopathy: rescue from death and prevention of dilated cardiomyopathy by chemokine receptor DNA therapy. J Immunol 2004, 173:3535–3541
6. Edwards RJ, Singleton AM, Boobis AR, Davies DS: Cross-reaction of antibodies to coupling groups used in the production of anti-peptide antibodies. J Immunol Methods 1989, 117:215–220
7. Matsumoto Y, Jee Y, Sugisaki M: Successful TCR-based immunotherapy for autoimmune myocarditis with DNA vaccines after rapid identification of pathogenic TCR. J Immunol 2000, 164:2248–2254
8. Kim G, Tanuma N, Kojima T, Kohyama K, Suzuki Y, Kawazoe Y, Matsumoto Y: CDR3 size spectratyping and sequencing of spectratype-derived T cell receptor of spinal cord T cells in autoimmune encephalomyelitis. J Immunol 1998, 160:509–513
9. Lehmann PV, Forsthuber T, Miller A, Sercarz EE: Spreading of T-cell autoimmunity to cryptic determinants of an autoantigen. Nature 1992, 358:155–157
10. McRae BL, Vanderlugt CL, Dal Canto MC, Miller SD: Functional evidence for epitope spreading in the relapsing pathology of experimental autoimmune encephalomyelitis. J Exp Med 1995, 182:75–85
11. Miller SD, Vanderlugt CL, Begolka WS, Pao W, Yauch RL, Neville KL, Katz-Levy Y, Carrizosa A, Kim BS: Persistent infection with Theiler's virus leads to CNS autoimmunity via epitope spreading. Nat Med 1997, 3:1133–1136
12. Vanderlugt CL, Neville KL, Nikcevich KM, Eagar TN, Bluestone JA, Miller SD: Pathologic role and temporal appearance of newly emerging autoepitopes in relapsing experimental autoimmune encephalomyelitis. J Immunol 2000, 164:670–678
13. Naserke HE, Ziegler AG, Lampasona V, Bonifacio E: Early development and spreading of autoantibodies to epitopes of IA-2 and their association with progression to type 1 diabetes. J Immunol 1998, 161:6963–6969
14. Li N, Aoki V, Hans-Filho G, Rivitti EA, Diaz LA: The role of intramolecular epitope spreading in the pathogenesis of endemic pemphigus foliaceus (fogo selvagem). J Exp Med 2003, 197:1501–1510
15. Bischof F, Bins A, Durr M, Zevering Y, Melms A, Kruisbeek AM: A structurally available encephalitogenic epitope of myelin oligodendrocyte glycoprotein specifically induces a diversified pathogenic autoimmune response. J Immunol 2004, 173:600–606
16. Warraich RS, Dunn MJ, Yacoub MH: Subclass specificity of autoantibodies against myosin in patients with idiopathic dilated cardiomyopathy: pro-inflammatory antibodies in DCM patients. Biochem Biophys Res Commun 1999, 259:255–261
17. Baba A, Yoshikawa T, Chino M, Murayama A, Mitani K, Nakagawa S, Fujii I, Shimada M, Akaishi M, Iwanaga S, Asakura Y, Fukuda K, Mitamura H, Ogawa S: Characterization of anti-myocardial autoantibodies in Japanese patients with dilated cardiomyopathy. Jpn Circ J 2001, 65:867–873
18. Caforio AL, Mahon NJ, Tona F, McKenna WJ: Circulating cardiac autoantibodies in dilated cardiomyopathy and myocarditis: pathogenetic and clinical significance. Eur J Heart Fail 2002, 4:411–417
19. Staudt A, Bohm M, Knebel F, Grosse Y, Bischoff C, Hummel A, Dahm JB, Borges A, Jochmann N, Wernecke KD, Wallukat G, Baumann G, Felix SB: Potential role of autoantibodies belonging to the immunoglobulin G-3 subclass in cardiac dysfunction among patients with dilated cardiomyopathy. Circulation 2002, 106:2448–2453
20. Staudt A, Staudt Y, Dorr M, Bohm M, Knebel F, Hummel A, Wunderle L, Tiburcy M, Wernecke KD, Baumann G, Felix SB: Potential role of humoral immunity in cardiac dysfunction of patients suffering from dilated cardiomyopathy. J Am Coll Cardiol 2004, 44:829–836
21. Müller J, Wallukat G, Dandel M, Bieda H, Brandes K, Spiegelsberger S, Nissen E, Kunze R, Hetzer R: Immunoglobulin adsorption in patients with idiopathic dilated cardiomyopathy. Circulation 2000, 101:385–391
22. Larsson L, Mobini R, Aukrust P, Gullestad L, Wallukat G, Waagstein F, Fu M: Beneficial effect on cardiac function by intravenous immunoglobulin treatment in patients with dilated cardiomyopathy is not due to neutralization of anti-receptor autoantibody. Autoimmunity 2004, 37:489–493

ARTHRITIS & RHEUMATISM
Vol. 56, No. 4, April 2007, pp 1304–1314
DOI 10.1002/art.22521

A New Murine Model to Define the Critical Pathologic and Therapeutic Mediators of Polymyositis

Takahiko Sugihara,[1] Chiyoko Sekine,[2] Takashi Nakae,[3] Kuniko Kohyama,[4] Masayoshi Harigai,[5] Yoichiro Iwakura,[6] Yoh Matsumoto,[4] Nobuyuki Miyasaka,[5] and Hitoshi Kohsaka[1]

Objective. **To establish a new murine model of polymyositis (PM) for the understanding of its pathologic mechanisms and the development of new treatment strategies.**

Methods. **C protein–induced myositis (CIM) was induced by a single immunization of recombinant human skeletal C protein in C57BL/6 mice, as well as in CD4-depleted, CD8-depleted, and mutant mice as controls. Some mice were treated with high-dose intravenous immunoglobulin (IVIG) after disease induction. Muscle tissues were examined histologically.**

Results. **In mice with CIM, inflammation was confined to the skeletal muscles. Histologic examination revealed a common pathologic feature of CIM and PM, involving abundant infiltration of CD8 and perforin-expressing cells in the endomysial site of the injured muscle. Suppression of myositis was achieved by depletion of both CD4 and CD8 T cells. Despite the development of serum anti–C protein antibodies in wild-type mice, severe myositis was induced in mice deficient in B cells. Induction of myositis was suppressed in interleukin-1α/β (IL-1α/β)–null mutant mice, but not in tumor necrosis factor α (TNFα)–null mutant mice. Use of IVIG, a treatment with proven efficacy in PM, suppressed CIM in the subgroup of treated mice.**

Conclusion. **CIM mimics PM pathologically and clinically. Infiltration of CD8 T cells is the most likely mechanism of muscle injury, and IL-1, but not B cells or TNFα, is crucial in the development of CIM. IVIG has therapeutic effects in CIM, suggesting that the effects of IVIG are not mediated by suppression of antibody-mediated tissue injury. This murine model provides a useful tool for understanding the pathologic mechanisms of PM and for developing new treatment strategies.**

Polymyositis (PM) is a chronic autoimmune inflammatory myopathy affecting striated muscles (1). Damage of muscles results in varying degrees of muscle weakness. Dysphagia with choking episodes and respiratory muscle weakness can occur in acute cases of PM. Currently, the pathogenesis of PM is unknown, and patients are therefore treated with nonspecific immunosuppressants. High-dose corticosteroids are the first-line treatment but are not effective in all patients. Improvement of disease often depends on the dosage of corticosteroids, making a dosage reduction difficult and thus, in many cases, necessitating administration of methotrexate or other immunosuppressants as adjunctive treatment. Because these medications can elicit a wide variety of adverse drug reactions, new therapies to address the specific pathologic features of PM are needed.

In affected muscles of patients with PM, infiltration of mononuclear cells leads to muscle fiber necrosis. These cells are found in the endomysial site, where non-necrotic muscle fibers are damaged, and also in the perimysial and perivascular sites of the muscles. Immunohistochemical studies have disclosed that CD8 T cells are most abundant in the endomysial site and invade

Supported by grants-in-aid from the Japanese Ministry of Education, Culture, Sports, Science, and Technology and from the Japanese Ministry of Health, Labor and Welfare.

[1]Takahiko Sugihara, MD, Hitoshi Kohsaka, MD, PhD: Tokyo Medical and Dental University, Tokyo, Japan, and Research Center for Allergy and Immunology, RIKEN, Yokohama, Japan; [2]Chiyoko Sekine, PhD: Research Center for Allergy and Immunology, RIKEN, Yokohama, Japan; [3]Takashi Nakae: Benesis Corporation, Osaka, Japan; [4]Kuniko Kohyama, MS, Yoh Matsumoto, MD, PhD: Tokyo Metropolitan Institute for Neuroscience, Tokyo, Japan; [5]Masayoshi Harigai, MD, PhD, Nobuyuki Miyasaka, MD, PhD: Tokyo Medical and Dental University, Tokyo, Japan; [6]Yoichiro Iwakura, DSc: University of Tokyo, Tokyo, Japan.

Address correspondence and reprint requests to Hitoshi Kohsaka, MD, PhD, Department of Medicine and Rheumatology, Graduate School, Tokyo Medical and Dental University, 1-5-45 Yushima, Bunkyo-ku, Tokyo 113-8519, Japan. E-mail: kohsaka.rheu@tmd.ac.jp.

Submitted for publication March 31, 2006; accepted in revised form January 16, 2007.